



## Probability distributions of non-structural carbon ages and transit times provide insights in carbon allocation dynamics of mature trees

|                               |   |
|-------------------------------|---|
| Journal:                      | <i>New Phytologist</i>  |
| Manuscript ID                 | NPH-MS-2019-31661.R1  |
| Manuscript Type:              | MS - Regular Manuscript   |
| Date Submitted by the Author: | n/a   |
| Complete List of Authors:     | Herrera, David; Max-Planck-Institut für Biogeochemie, Biogeochemical Processes<br>Muhr, Jan; Max-Planck Institute for Biogeochemistry, Biogeochemistry<br>Hartmann, Henrik; MPI for Biogeochemistry, Forest Ecology and Ecophysiology<br>Römermann, Christine; Friedrich-Schiller-Universität Jena, Plant Biodiversity Group, Institute of Systematic Botany; German Centre for Integrative Biodiversity Research (iDiv) Halle-Jena-Leipzig, Biodiversity research; Universität Regensburg, Institute of Botany, Theoretical Ecology<br>Trumbore, Susan; Max-Planck-Institute for Biogeochemistry, Biogeochemical Processes<br>Sierra, Carlos; Max Planck Institute for Biogeochemistry, Biogeochemical Processes |
| Key Words:                    | Carbon allocation, Non-structural carbohydrates, Tree storage dynamics, Carbon ages and transit times, Tree carbon dynamics, Modeling   |
|                               |   |

1     **Probability distributions of non-structural carbon ages and transit times provide**  
2     **insights in carbon allocation dynamics of mature trees**

3                             David Herrera-Ramirez<sup>1\*</sup>

4                             Jan Muhr<sup>1,2</sup>

5                             Henrik Hartman<sup>1</sup>

6                             Christine Römermann<sup>3,4</sup>

7                             Susan Trumbore<sup>1</sup>

8                             Carlos A. Sierra<sup>1</sup>

9     <sup>1</sup>Max Planck Institute for Biogeochemistry, Hans-Knöll-Str 10, 07745 Jena

10    <sup>2</sup>Georg August University Göttingen, Department of Bioclimatology, Büsgenweg 2,  
11    37077 Göttingen, Germany

12    <sup>3</sup>Friedrich Schiller University Jena, Institute for Ecology and Evolution, Philosophenweg  
13    16, 07743, Jena, Germany

14    <sup>4</sup>German Centre for Integrative Biodiversity Research (iDiv) Halle-Jena-Leipzig, D-  
15    04103 Leipzig

16    \*Author for correspondence: David Herrera-Ramirez,

17    Email: dherrera@bgc-jena.mpg.de; Phone: +49 (0)3641 57-6152

18

19

20    Total word count: 7019; Introduction: 1183; Materials and Methods: 2188; Results: 1248;  
21    Discussion: 2400; Number of figures: 6; Figures in color: 3, 4, 5, 6; Number of tables: 4.

## Summary

- In trees, the use of non-structural carbon (NSC) under limiting conditions impacts the age structure of the NSC pools. We compared model predictions of NSC ages and transit times for *Pinus halepensis* Mill., *Acer rubrum* L. and *Pinus taeda* L., to understand differences in carbon storage dynamics in species with different leaf phenology and growth environments.
- We used two carbon allocation models from the literature to estimate the NSC age and transit time distributions, to simulate carbon limitation, and to evaluate the sensitivity of the mean ages to changes in allocation fluxes.
- Differences in allocation resulted in different NSC age and transit time distributions. The simulated starvation flattened the NSC age distribution and increased the mean NSC transit time, which can be used to estimate the age of the NSC available and the time it would take to exhaust the reserves. Mean NSC ages and transit times were sensitive to carbon fluxes in roots and allocation of carbon from wood storage.
- Our results demonstrate how trees with different storage traits are expected to react differently to starvation. They also provide a probabilistic explanation for the “last-in, first-out” pattern of NSC mobilization from well-mixed carbon pools.

## Keywords

Carbon allocation, non-structural carbohydrates, tree storage dynamics, carbon ages and

transit times, tree carbon dynamics, modeling.

**Introduction**

The availability and mobility of the non-structural carbon (NSC) reserves, mostly sugars and starch, determine trees' ability to survive photosynthetic shortages (Dietze *et al.*, 2014; Hartmann & Trumbore, 2016; Martínez-Vilalta *et al.*, 2016; Overdieck, 2016; Trugman *et al.*, 2018; Wiley *et al.*, 2019). Carbon limitation may occur due to stresses such as droughts, physical damage, pests, diseases, and floods, that may become more frequent due to climatic changes (IPCC, 2018; Klein & Hartmann, 2018). Tree mortality associated with these stressful conditions (Bréda *et al.*, 2006; Carnicer *et al.*, 2011; von Arx *et al.*, 2017) may cause biodiversity loss (Nunez *et al.*, 2019), economic losses (Strand, 2017; Oliveira *et al.*, 2019) and long-term modifications to the global carbon cycle (McDowell *et al.*, 2018; Pugh *et al.*, 2019). Under stress, trees mobilize NSC from storage to sustain metabolic and growth requirements (Anderegg & Anderegg, 2013; Klein & Hoch, 2015; Mei *et al.*, 2015). Although carbon allocation has been widely investigated during the last decades, it is a complex process that is still not fully understood (Hartmann & Trumbore, 2016). In general, carbon fixed during photosynthesis is transported as NSC from chloroplasts to different plant organs (e.g., leaves, branches, stems, and roots) where it is allocated either to metabolism (respiration, growth, defense, osmotic regulation, among others) or to storage, which may occur passively or actively (Lacointe *et al.*, 2004; Wiley *et al.*, 2013; Huang *et al.*, 2019b). To represent and understand these dynamics, compartmental models have been proposed

where NSC is allocated to both organ specific compartments (e.g., leaves, stems and roots) and compound specific compartments (Richardson *et al.*, 2012; Klein & Hoch, 2015; Ceballos-Núñez *et al.*, 2018).

One example of recent advances is the observation that the  $^{14}\text{C}$ -modeled mean age of NSC in tree stems increases with depth in the stem. This has been modeled in two ways. Richardson *et al.* (2015) proposed a two pool model of NSC with ‘active’ (< 1 year old) labile carbon that is quickly cycled through the tree and replenished mostly by the influx of newly assimilated carbon and ‘stored’, older NSC that accumulates when photosynthesis surpasses demand and is retrieved at slow rates. These two compartments have been associated with specific compounds -sugar and starch- (Klein & Hoch, 2015). However, the similar ages reported for sugar and starch pools using  $^{14}\text{C}$  do not support this generalization (Richardson *et al.*, 2015). Despite recent efforts, it is still difficult to differentiate and measure fast and slow cycling pools of NSC in trees. Alternatively, Trumbore *et al.*, (2015) explained the increasing ages of NSC with depth in stem-wood by transport, using a simple diffusion model of one NSC compartment and radial mixing of mobile carbon of different ages. In this model, the net mixture of NSC inwards from the phloem along rays is a source of NSC that is younger than the structural C where it is found. The ability of different models to explain the same observation indicates the importance of a model representation of carbon allocation for improving our ability to estimate and understand NSC dynamics.

In trees, NSC dynamics determine the age and transit time distributions of the carbon in the different organ specific and compound specific pools (Ceballos-Núñez *et al.*, 2018). Carbon age is defined as the time elapsed since a carbon atom enters the system until the

89 time of observation (Bolin & Rodhe, 1973), i.e., an age of zero represents the moment of  
90 carbon fixation from the atmosphere. Transit time is defined as the time that a carbon  
91 atom remains in the system until it exits (Ceballos-Núñez *et al.*, 2018). To give an  
92 example: when defining our observed system as all the NSC in a tree, carbon atoms  
93 would enter through photosynthesis (with age equal to zero) and leave when being  
94 allocated to the formation of structural tissue (growth) or to catabolic requirements (e.g.,  
95 loss as CO<sub>2</sub>). Here, we define NSC transit time as the time elapsed between these two  
96 points. These definitions allow us to estimate the distributions of the NSC ages and NSC  
97 transit times across all carbon pools using models (Ceballos-Núñez *et al.*, 2018; Metzler  
98 *et al.*, 2018). This offers a useful alternative to evaluate NSC dynamics in trees. While the  
99 precise measurement of these quantities remains elusive, the mean age and mean transit  
100 time of the NSC of different organs have been estimated from <sup>14</sup>C measurements in the  
101 sugars and the respired <sup>14</sup>CO<sub>2</sub>, respectively, and by pulse labeling techniques in trees  
102 (Carbone *et al.*, 2006, 2013; Epron *et al.*, 2012; Trumbore *et al.*, 2015; Muhr *et al.*, 2016,  
103 2018).

104 For healthy, unstressed trees not experiencing carbon limitation NSC in respiration and  
105 growth consists mainly of carbon from the current growth year (< 1 year old)  
106 (Richardson *et al.*, 2015; Muhr *et al.*, 2018). However, previous studies have shown that  
107 trees under C supply limitation start mobilizing stored carbon, resulting in an increase in  
108 the mean age of the C used for new growth or metabolism (Vargas *et al.*, 2009; Carbone  
109 *et al.*, 2013; Trumbore *et al.*, 2015; Ceballos-Núñez *et al.*, 2018; Muhr *et al.*, 2018). How  
110 the quantity and mobility of stored carbon varies with tree species and/or between organs  
111 in the same tree will result in different age and transit time distributions. To date, we lack

systematic understanding about how NSC age distributions differ between tree organs and tree species, and about the differences in the use of the NSC reserves under outstanding carbon limitation. To answer these questions, and to test hypotheses about C allocation strategies in trees, it is important to have the ability to estimate NSC age and transit time distributions.

The representation of carbon allocation in compartmental systems allows such estimation of NSC age and transit time distributions (Ceballos-Núñez *et al.*, 2018; Metzler *et al.*, 2018; Metzler & Sierra, 2018). These distributions describe the relative abundance of carbon of different ages in each NSC pool. By compartmentalizing two whole-tree carbon allocation models proposed by Klein & Hoch (2015) and Ogle & Pacala (2009), and estimating the age and transit time distributions based on the mathematical framework developed by Metzler & Sierra (2018) and Metzler *et al.* (2018), we address here three main questions: **i)** How different are the predictions of NSC dynamics overall and between tree organs, for contrasting plant types (evergreen vs. deciduous) or for contrasting environmental conditions (severe growth limitations vs. favorable conditions)? **ii)** What is the predicted age structure of the NSC reserves available and how long, theoretically, trees would take to consume these reserves? And **iii)** what are the principal carbon fluxes that influence the NSC mean ages and mean transit times? We expect that compartmental models, which consider organ specific and compound specific carbon pools, will allow us to estimate differences in the NSC age distributions of trees with different life strategies, and to associate them with different storage traits. We also expect that, by estimating the changes of the NSC transit time during a severe carbon limitation, we can describe the age structure of the carbon available for sustaining the

tree's metabolism and growth and to estimate how long it can take for the trees to exhaust their reserves.

## Materials and Methods

### Model descriptions

We used compartmental linear models of carbon allocation in individual trees to estimate NSC age and transit time distributions (Figs. 1 and 2). We used species of different leaf phenology -evergreen and deciduous- and different growth environments, Mediterranean and temperate forest. Compartmental models describe the exchange of mass between compartments following mass conservation principles (Jacquez & Simon, 1993; Metzler & Sierra, 2018). This means that: i) the mass of NSC leaving each compartment is a fraction of the mass of the NSC compartment, and ii) the mass entering the compartment is immediately mixed with the mass of the NSC compartment, making the mass of the compartment homogeneous at any time (Metzler & Sierra, 2018). The structure of the compartmental linear models follow those described in Klein & Hoch (2015) for *Pinus halepensis* Mill. and on Ogle & Pacala (2009) for *Acer rubrum* L. and *Pinus taeda* L. with small variations based on theoretical assumptions (Figs. 1 and 2). We estimated the model parameters (annual fraction of carbon transferred between pools) based on the carbon fluxes and pool stocks reported in the two studies for each species (Tables 2 and 1).

The model proposed by Klein & Hoch (2015) was parameterized using a carbon balance approach and exhaustive eco-physiological measurements during more than 13 years at Yatir forest, Israel. *P. halepensis* occurs in humid Mediterranean regions, but Yatir forest



is a semi-arid forest with only 285 mm of annual precipitation and an extended drought period of several months, so trees there are at the limit of the species' growth requirements (Klein & Hoch, 2015). Model parameters were estimated for a typical mature and healthy tree where the amount of carbon fixed was assumed to be very close to the amount of carbon released, i.e., trees were close to a steady state condition with respect to carbon (Klein & Hoch, 2015). Three organ specific carbon pools were defined as: stem, foliage and belowground; each with three compound specific carbon pools: starch (stored NSC), soluble sugars (active NSC) and structural carbohydrates (i.e., biomass) (Fig. 1). In the original model, the starch and soluble sugars were categorized into stored (slow cycling) and active (fast cycling) NSC pools, respectively. All fluxes of carbon were reported in the original publication in grams of carbon per tree per day (gC d<sup>-1</sup>) and converted to grams of carbon per tree per year (gC yr<sup>-1</sup>). Then, we calculated the annual fraction of carbon that leaves each pool (yr<sup>-1</sup>). i.e. the ratio of flux divided by pool size of the donor pool. These fractions were used as the parameters for the model (Fig. 1 and Table 2).

Ogle and Pacala (2009) proposed a mechanistic model named "Allometrically Constrained Growth and Carbon Allocation" (ACGCA). We used the ACGCA model to estimate the fluxes and pool sizes of the model in Figure 2 for a typical mature and healthy tree of both species *A. rubrum* and *P. taeda* at steady state (Table 2). The parameters for steady state were obtained after running the ACGCA model for 700 time steps, to the point where pool sizes and fluxes did not change with time. ACGCA estimates the pool stocks in grams of glucose per tree (gGluc) and the fluxes in grams of glucose per tree per year (gGluc yr<sup>-1</sup>). Here, we converted these parameter values to

grams of carbon (gC) and grams of carbon per year (gC yr<sup>-1</sup>) respectively, based on the molar masses of carbon and glucose (12 and 180.15 g mol<sup>-1</sup>, respectively). Then, the model parameters were also calculated by dividing the flux value by the size of the compartment from which C was removed, obtaining the annual fraction of carbon leaving each pool.

The ACGCA model was designed to estimate growth and reproduce a range of physiological states defined by tree's allometries and labile carbon (NSC) status (Ogle & Pacala, 2009). The model we used for our estimations and simulations follows a linear compartmental interpretation of the ACGCA model. This model is structurally similar to the one used for *P. halepensis*: It considers organ specific carbon pools as foliage, branches and coarse roots, stem, and fine roots; and compound specific carbon pools as transient NSC, active NSC, stored NSC, and structural carbohydrates per tree organ (Fig. 2). Nevertheless, the chemical nature of the carbon in these pools is restricted to glucose; no differentiation between starch and sugar is made.

These models were described with a system of ordinary differential equations expressed in the general linear non-autonomous form presented in Ceballos-Núñez *et al.*, (2018):

$$\frac{dx(t)}{dt} = B \cdot x(t) + b \cdot u(t), \quad x(t = 0) = x_0, \quad (1)$$

where  $\frac{dx(t)}{dt}$  is the vector of rates of change of carbon with respect to time in each compartment; B is a  $m \times m$  square matrix where m is the number of compartments in the model, the diagonal elements of the matrix are the fraction of carbon leaving each pool and the off-diagonal entries represent the fraction of carbon transferred among compartments;  $x(t)$  is the vector of mass of carbon in each compartment; b is the vector

of partitioning of the photosynthetic input  $u(t)$ ; and  $x_0$  is a vector of initial values of the carbon compartments.

#### **Estimation of NSC ages and transit times of mature healthy trees (close to steady state)**

The description of the models in the system of differential equations (Equation 1) allowed us to estimate the age and transit time distributions at steady state for each species. Here, we interpret steady state as the condition of mature and healthy trees whose carbon uptake is nearly balanced by respiration and litter fall. These distributions were calculated as the sum of exponential distributions using the formulas developed by Metzler & Sierra (2018). The age density distribution of the carbon that is in the system is given by the probability of finding carbon particles of a certain age  $y \geq 0$  ( $f_A(y)$ ) and it follows the equation

$$f_A(y) = z^T \cdot e^{y \cdot B} \cdot \frac{x^*}{\|x^*\|}, \quad y \geq 0, \quad (2)$$

where  $z^T$  is the vector of release rates from the system,  $e^{y \cdot B}$  is the matrix exponential evaluated at age  $y$ , and interpreted as the probability matrix of transfers among compartments,  $\frac{x^*}{\|x^*\|}$  is the distribution of carbon among the different pools, and  $x^*$  is the steady-state content of the system (Equation 1). We use here the symbol  $\|\cdot\|$  to represent the vector norm, which is the sum of the absolute values of all entries of the vector.

The mean age is given by the expected value ( $E[A]$ )

$$E[A] = \frac{\|B^{-1} \cdot x^*\|}{\|x^*\|}. \quad (3)$$

Transit time can be considered as forward transit time (FFT) or backward transit time (BTT) (Metzler *et al.*, 2018). The FFT is the time a particle would take to travel the system after its arrival at a given time. The BTT is the age that a particle has when it leaves the system. Therefore, the BTT density distribution ( $f_{\text{BTT}}(y)$ ) describes the probability that a carbon particle has a certain age  $y$  when it leaves the system at time  $t$ . As our aim concerns the age of the carbon when it leaves the system as respired  $\text{CO}_2$ , we will deal here with the BTT only expressed as:

$$f_{\text{BTT}}(y) = z^T \cdot e^{y \cdot B} \cdot \beta, \quad y \geq 0. \quad (4)$$

The mean backward transit time is defined as ( $E[\text{BTT}]$ ):

$$E[\text{BTT}] = \frac{\|x^*\|}{\|u\|}. \quad (5)$$

Note that the definitions presented here can only be applied to autonomous systems at steady state (Metzler & Sierra, 2018). Therefore, these formulas were used to characterize the NSC dynamics of mature and healthy trees where the carbon inflow  $u$  and the coefficients in  $B$  do not change over time. To characterize NSC dynamics, the age and transit time distributions were calculated only for the NSC pools of the described models in Figs. 1 and 2.

### **Estimation of NSC ages and transit times of trees under carbon source limitation (out of steady state)**

We estimated time-dependent NSC age and transit time distributions for 40 years after the assimilation input ( $u(t)$ ) was set to zero ( $f_A(y,t)$ ,  $f_{\text{BTT}}(y, t)$ ), while keeping the transfer carbon coefficients (matrix  $B$ ) constant. We used zero assimilation to have a clear view of

how trees use their NSC when they depend exclusively on storage. This approach allowed us to evaluate how limitations in carbon assimilation would impact the age and transit time distributions of carbon in mature and healthy trees. The changes in these quantities reflect the age of remaining NSC reserves and the age of carbon used for respiration at each time step under carbon limitation.

In our simulations, we kept the assimilation flux  $u(t)$  constant at the levels reported for healthy trees in steady state (Table 2) for the first 10 years ( $t < t_0$ ), and then set it to zero in any subsequent time  $t \geq t_0$  until  $t=50$ . Until  $t_0$ , the NSC age and transit time distributions  $f_A(y)$  and  $f_{BT}(y)$  did not change. These distributions constitute the initial (steady state) conditions for the system prior to the carbon limitation. The mathematical framework for estimating the age and transit time distributions when the elements of the system (Equation 1) depend on time, and are out of steady state, was developed by Metzler *et al.*, (2018). The approach consists of solving the system of differential equations (Equation 1) first, and then take this solution to reconstruct an analogous linear system of differential equations with the same solution trajectory. From the new system, it is possible to obtain a mathematical object called the state transition operator, which encapsulates all the dynamics of the system, including the probabilities of carbon particles moving from one pool to another. Since we know the initial age distributions from the steady-state system, we use the state transition operator to move the initial age distribution forward in time. We therefore estimated the NSC age and transit time distributions and their respective mean values for the subsequent times  $t > t_0$ . We calculated the percentage of the NSC consumed in each time step after the carbon limitation started by computing the solutions of each model (Equation 1) for each time

step, which gives us the amount of the NSC remaining in each carbon pool, and then subtracting this quantity from the initial amount of NSC in the system. We used the python packages “bgc-md” and “CompartmentalSystems”, which implement the formulas required for these computations (Metzler *et al.*, 2018).

### **Sensitivity and uncertainty of the NSC mean age and mean transit time to variations in sink strength**

To understand the sensitivity of the NSC mean age and mean transit time at steady state to changes in the sink carbon fluxes, we evaluated the change in NSC mean age and mean transit time to a given numerical alteration of the fraction of carbon leaving each pool (coefficients of matrix B in Equation 1). This analysis allowed us to identify the pool-specific fluxes that have the greatest influence on the overall NSC ages and transit times in mature trees. For that, we used the method “Elementary Effects” (Morris, 1991; Campolongo *et al.*, 2007). This method analyzes the change in model output if exactly one parameter ( $p_i$ ) is changed by a random fraction ( $dp_i$ ) between L levels (150) in the parameter space. The parameter space was estimated based on the parameter variability provided by Klein & Hoch (2015) and Ogle & Pacala (2009) (Table 2). It then changes each parameter once and repeats this process throughout  $p$  (parameters) +1 simulations that are called a “trajectory” (Cuntz *et al.*, 2015). Then, we ran 100 trajectories. We estimated a bigger parameter space than the one reported for each species to capture a more general trend outside of the limits of each species. Then, the Elementary Effect of each parameter  $EE_i$  in each trajectory is calculated as a differential quotient

$$EE_i = \frac{f(p_i + dp_i) - f(p_i)}{\delta}, \quad (6)$$

where  $\delta$  is  $dp_i$  as a fraction of the  $dp_i$  range. The mean  $\mu^*$  and the variance  $\sigma$  of the absolute values of the  $EE_i$  from the 100 trajectories were used as a measure of sensitivity (Cuntz *et al.*, 2015). The Elementary Effects simulations and calculations were done using the R packages “sensitivity V1.15.2” (Pujol *et al.*, 2017) and “SoilR” (Sierra *et al.*, 2014).

To evaluate how the uncertainty in the models’ parameters affects the mean age and the mean transit time of the species evaluated, a Monte Carlo Simulation (MCS) analysis was performed. This method involves repeated model realizations of a random selection of parameter values (Parkinson & Young, 1998). The standard deviation associated with each parameter has been derived from Klein & Hoch (2015) for *P. halepensis* and from Ogle & Pacala (2009) for *A. rubrum* and *P. taeda* (Table 2). Then we ran 1000 MCSs for estimating the corresponding standard deviation of the mean age and mean transit time of the NSC for the whole tree and for each carbon pool. Just the most influential parameters of each model were re-sampled assuming they come from independent Gaussian distributions. This assumption of independence is potentially limiting given that the MCS analysis would yield different results if there were covariance between the parameters. However, the degree of association between parameters is unknown to us. If better information on their correlation would be available, this uncertainty could be re-estimated.

## 307     **Results**

### 308     **NSC ages and transit times of mature healthy trees (trees close to steady state)**

309     Different tree species of contrasting functional types had distinct NSC age and transit  
 310     time distributions (Figs. 3 and 5). For simplicity, we use the mean values of these  
 311     distributions to describe these differences here. For *P. halepensis*, the mean NSC transit  
 312     time - the age of carbon being used in metabolism and growth- was very young ( $0.49 \pm$   
 313      $0.08$  years). Likewise, the overall mean NSC age (the age of the carbon remaining in the  
 314     tree) was also very young ( $0.98 \pm 0.38$  years). In contrast, the temperate species *A.*  
 315     *rubrum* and *P. taeda* had slower predicted carbon cycling with mean ages of  $9.45 \pm 3.7$   
 316     and  $4.4 \pm 0.72$  years and transit times of  $2.95 \pm 0.31$  and  $2.4 \pm 0.09$  years, respectively.

317     The predicted NSC age and transit time distributions among different carbon pools  
 318     showed contrasting behaviors. NSC age distributions for all the NSC pools in *P.*  
 319     *halepensis* were similar across tissues (Fig. 3 and Table 3). For this species, the NSC  
 320     stored in stem and roots had the oldest mean ages (Table 3). In contrast, there was a clear  
 321     distinction in the predicted mean ages of active and stored NSC pools for the temperate  
 322     species *A. rubrum* and *P. taeda* (Table 3). The NSC stored in the stem had a mean age of  
 323      $21.3 \pm 5.38$  years in *A. rubrum*, but only  $14.2 \pm 1.63$  years in *P. taeda*. The mean ages of  
 324     NSC stored in the foliage and fine roots (FSNSC and RSNSC pools) were lower in *A.*  
 325     *rubrum* ( $3.5 \pm 0.20$  and  $2.5 \pm 0.20$  years respectively) than in *P. taeda* ( $5.2 \pm 0.06$  and  
 326      $4.19 \pm 0.06$  years, respectively, Table 3). In general, the age of the NSC in leaves was  
 327     greater than we expected, especially in the deciduous tree *A. rubrum*. Overall, the age of  
 328     the NSC in each tree organ is given by the combination of the NSC ages of the compound



specific compartments -active, stored and transient NSC pools- in each respective organ. Mean age estimates of the NSC in leaves and fine roots are less than two years (Table 4). In the stem, mean ages of NSC were  $0.73 \pm 0.58$ ,  $9.97 \pm 5.38$  and  $4.58 \pm 1.63$  years for *P. halepensis*, *A. rubrum* and *P. taeda* respectively (Table 4).

NSC age and transit time distributions characterized in detail the age composition of the NSC that remains in and leaves the tree (Figs. 3 and 5). The mixture of NSC ages for mature healthy trees followed a phase type distribution (Fig. 3), which is a mixture of exponential distributions (Metzler & Sierra, 2018). The shape of the distributions depended on the speed at which the carbon was cycled within the tree. Carbon age distributions allowed us to better understand the age composition of each carbon pool. For instance, for *P. halepensis*, 95% of all NSC in the entire tree was younger than 3.3 years. For *A. rubrum*, 95% of the NSC was less than 42 years old, and NSC respired or allocated to growth did not exceed 2.9 years. In *P. taeda*, 95% of all NSC was less than 20 years old, while 95% of the NSC leaving the system was younger than 2.4 years old. The trees' NSC pools had different NSC age and transit time compositions (Figs. 3 and 5), which characterize the different dynamics of each NSC compartment in the trees' carbon balance.

#### **NSC ages and transit times of trees under carbon source limitation (out of steady state)**

When simulating carbon limitation for the trees characterized in Fig. 3, our model predicted changes in the shape of the NSC age and transit time distributions over time due to NSC storage mobilization (Figs. 4 and 5). The simulated carbon limitation

progressively reduced the mass of NSC in storage compartments (Fig. 4). The carbon mass drawn from storage was younger during the initial phase of the simulations and increased during the simulations (Fig. 5). The proportion of young carbon decreased rapidly, flattening the entire NSC age distribution of the trees (Fig. 4). Consequently, both the mean age and mean transit time of the NSC increased as carbon limitation progressed. The mean transit time increased first in an exponential way and then linearly (Fig. 6). The exponential phase reflects the progressive and fast depletion of young reserves and increasing importance but slower utilization of old carbon. Then, when the age distribution of the remaining NSC becomes increasingly uniform, the linear phase describes the aging of the remaining carbon.

The increase in mean transit time during carbon limitation indicates that trees used increasingly older reserves for respiration as the storage pool was exhausted. For trees that can store carbon for a longer time, such as *A. rubrum* and *P. taeda*, the cessation of assimilation resulted in an increase in the mean transit time of several years, due principally to the availability of several decades old NSC in the stem and coarse roots to support metabolism (Fig. 3). For *A. rubrum*, the mean transit time increased from  $2.9 \pm 0.31$  years in healthy conditions to  $10.3 \pm 0.31$  years when trees had consumed 50-60% of the reserves, and to  $21 \pm 0.31$  years when only 20% of their reserves remained (Fig. 6). For *P. taeda*, mean transit times increased from  $2.4 \pm 0.09$  years at steady state to  $5 \pm 0.09$  years (50-60% consumption), and to  $13 \pm 0.09$  years (80% consumed) (Fig. 6). For *P. halepensis* trees growing in Yatir forest, the transit time increased from  $0.48 \pm 0.08$  years to  $4 \pm 0.08$  years at the end of the exponential trend (Fig. 6).

## **Sensitivity and uncertainty of mean age and mean transit time to variations in sink strength**

The mean age was mainly sensitive to changes in the consumption of NSC from stored carbon in the stem, branches and coarse roots (Cs) and the loss of NSC in the transition from sapwood to heartwood (LSs) (Fig. S2). The mean transit time was principally sensitive to the allocation of NSC to storage in the roots (Sr and Sbr) and root growth (Gr). In addition, both quantities were sensitive to changes in the allocation to root active NSC (Stor and BRI), and to a lesser degree, to root respiration (Rr) (Fig. S2). The impact of changes in these cycling rates on the mean age and mean transit time is complex and non-linear in some cases as indicated by high variance of the sensitivity index (Figs. S2 and S3). But in general, the higher the consumption from the NSC stem pools, the younger the NSC in the tree; and the greater the storage of NSC in the roots, the older the NSC in the tree.

The mean uncertainty (1.5 years) in the mean ages and transit times reflected uncertainties in the most influential cycling rates, as described above. This uncertainty was smaller than the mean differences between species (5.97 years). In general, *A. rubrum* had higher uncertainties than *P. taeda* and *P. halepensis* (Fig. S1). Some exceptionally high mean ages of the NSC could be obtained in very rare combinations of parameter values at the very limit of their distributions (Fig. S1).

## **Discussion**

The whole-tree compartmental models for carbon allocation tested here allowed us to estimate: i) differences in the NSC age and transit time distributions that reflected carbon

storage dynamics of different tree species; ii) the change in the age of the NSC used under carbon limitation; and iii) the main NSC cycling rates that influenced the NSC mean age and mean transit time in mature trees.

### ***NSC dynamics between tree tissues and tree species***

The predicted NSC age and transit time distributions indicated large differences between tree species that reflected differences in functional types: deciduous (*A. rubrum*) or evergreen (*P. taeda*); and growth environments: highly limited (Mediterranean *P. halepensis*) and mesic growth conditions (temperate species) (Fig. 3). These differences reflected the locations where reserves accumulate, and how long they remain in each carbon pool. For instance, *A. rubrum* stored more old carbon, evidenced in the longer tail of the NSC age distribution, compared to *P. taeda* and *P. halepensis* (Fig. 3). The age distribution of NSC within each pool reflects the role of each NSC pool in carbon cycling and storage of mature trees. For temperate species, NSC was stored longer in the stem and coarse roots (SSNSC), with more old carbon present (Fig. 3). In contrast, *P. halepensis* did not show actual age differences between slow (stored NSC) and fast (active NSC) pools (Fig. 3) suggesting no capacity for long-term storage of NSC. However, it may also be possible that long-term storage pools were neglected by the assumptions made in this model (e.g. the fast and slow pools were associated with the sugar and starch compartments, respectively). These results demonstrate the difficulties of separating and measuring fast and slow cycling NSC pools, and highlight the utility of estimating NSC ages based on compartmental systems to identify and understand the carbon dynamics associated with these elusive carbon pools (Richardson *et al.* 2015). Despite the fact that our mean NSC age estimates in leaf compartments were almost one

year older than what has been reported previously (Keel *et al.*, 2007; Gaudinski *et al.*, 2009), our results predicted different carbon storage traits between tree species that range from slow carbon cycling trees that accumulate larger proportions of long term reserves (e.g., *A. rubrum*) and fast carbon cycling trees with low accumulation of long term reserves (e.g., *P. halepensis*).

NSC transit time distributions reflected the age composition of NSC reserves being used by trees in metabolism and growth. Our estimates showed that healthy trees used mainly young carbon (Fig. 5). The allocation of mainly young carbon to respiration and growth in mature healthy trees has been already documented (Carbone *et al.*, 2013; Muhr *et al.*, 2018). This behavior has been commonly explained by the “last in, first out” hypothesis for using the NSC where the most recently fixed carbon entering the systems is the one that is used at first (Dietze *et al.*, 2014; Hartmann & Trumbore, 2016). In our models, this idea is partly represented by the differentiation between fast and slow NSC cycling pools in each tissue. This differentiation in organ NSC pools and compound NSC pools (fast and slow cycling pools) represents the spatial heterogeneity of the NSC ages within the tree. Partly in disagreement with the ‘last in, first out’ principle, previous studies have also shown that some old NSC is mixed in the metabolized CO<sub>2</sub> in healthy trees with non-limiting assimilate supply, due to the continuous exchange of carbon between the active NSC and the stored NSC pools (Richardson *et al.*, 2012; Carbone *et al.*, 2013; Muhr *et al.*, 2013). This is in agreement with our results where the NSC transit time distributions (Fig. 5) showed that the carbon being used in metabolism and growth is a mixture of carbon of different ages. The transit time distribution is mainly determined by the age structure of the largest carbon source and the balance between carbon sources and

sinks in the tree. In this sense, in healthy-mature trees the inflow of new carbon greatly exceeds the retrieval of old stored carbon for sustaining metabolism and growth, which leads to the high abundance of young NSC in the trees and skewness of the distribution towards low values, with corresponding low values of mean transit time (Figs. 3 and 5). Therefore, within our framework, healthy trees may use mainly young carbon due to its high abundance in the NSC pools, and its constant replenishment due to rapid assimilation of atmospheric carbon, and not because the younger carbon is more available due to its position in the tree. This concept is supported by the simulation results in Fig. 4 where the young carbon is depleted faster than the old carbon -due to its relative high abundance -until eventually flattening the age distribution of the NSC in each pool.

In other words, our results provide a probabilistic interpretation for the use of young carbon for metabolism and growth. Since young NSC is more abundant in storage pools, it has a greater probability of being used for plant function. These results provide a new perspective on the understanding of the NSC allocation to metabolism and growth and also highlight the utility of obtaining the NSC transit time distribution in mature trees for understanding carbon source/sink imbalances.

#### ***Age structure of NSC reserves under carbon limitation***

Under severe carbon limitation, the modeled trees used their NSC reserves to support metabolic needs and consequently the NSC mean transit time increased rapidly (Fig. 6). Previous studies that interrupted carbon assimilation either by girdling, harvesting of the main trunk, or hurricane damage, also reported a rapid increase in the NSC mean transit

time from very young to several years old carbon. For instance,  $^{14}\text{CO}_2$  respired from *Scleronema micranthum*, a measure of transit time, increased from 1 to 15 years old over a year after girdling (Muhr *et al.*, 2018); stump resprouts in *A. rubrum* growing after trunk harvesting were found to be made of carbon up to 17 years old (Carbone *et al.*, 2013); and up to 10 years old carbon was used to grow new roots for tropical trees after a hurricane damage (Vargas *et al.*, 2009). In addition, D'Andrea *et al.*, (2019) reported that the mean age of sugars in the phloem of beech trees that were defoliated by frost late in spring increased to ca. 5 years within only few weeks.

We were able to describe how this old carbon was used and for how long it could last by observing how the NSC mean transit time increased over time during our simulations. The NSC mean transit time increased in an exponential way that depended on the amount and the cycling speed of the reserves, followed by a linear phase that occurred when the NSC age distribution got flat and only described the aging of the remaining NSC (Fig. 6). We observed that the exponential increase in the NSC mean transit time described how the trees consume between 80 and 90% of the available carbon, depending on their storage strategy (Fig. 6). The NSC mean transit times towards the end of the exponential increase was higher (14-21 years) than the reported (12-17 years) age of the respired  $\text{CO}_2$  of trees subjected to starvation (Carbone *et al.*, 2013; Muhr *et al.*, 2018). This difference can be explained by the fact that we did not represent mortality explicitly; therefore, the trees continued using reserves for a longer time than in experiments where the trees die before exhausting 80- 90% of their reserves. Considering a consumption threshold between 50 to 60% (Mei *et al.*, 2015; Wiley *et al.*, 2019), the mean transit time is 5 and 10 years for *P. taeda* and *A. rubrum*, respectively (Fig. 6), in accord with what has been

486 reported for starving trees. Our predictions also report a very slow consumption of the  
487 reserves when trees are under carbon limitation, taking between 2 to 5 years to exhaust  
488 80% of their reserves, and between 1 to 3 years to reach the 50-60% of NSC  
489 consumption. Measurements in mature trees documented an up to three times faster  
490 increase in the NSC mean transit time than in our model (Carbone *et al.*, 2013; Muhr *et*  
491 *al.*, 2018). These discrepancies between our model estimates and NSC ages reported in  
492 empirical studies, along with the unexpected high mean NSC ages in leaves, could be due  
493 to several reasons: i) The parameters provided for our models may not fully represent the  
494 trees evaluated in the studies; more precise and exhaustive parameter estimation may be  
495 needed; ii) the measurements may have been taken for trees that have not reached yet  
496 their steady state and therefore have higher transfer coefficients of carbon between pools;  
497 iii) additional fluxes and carbon compartments not considered in the model, plus other  
498 mechanisms not considered, such as: trees' ability to control growth and respiration under  
499 stress, active NSC allocation to storage, or other non-linearities in the model. Thus,  
500 alternative model structures may be needed; iv) our source limitation simulations were  
501 restricted only to a complete cease of carbon assimilation. Limiting conditions such as  
502 drought or severe physical damage, also may imply a limitation in the mobilization of the  
503 stored NSC or truncation of the NSC mass, which would reduce the quantity of stored  
504 NSC available and cause a quicker depletion of the NCS in the trees; and/or v)  
505 measurements of respired  $^{14}\text{CO}_2$  in previous studies is restricted to the stem-wood and  
506 thus do not reflect the time that the increase in the mean NSC transit time would take for  
507 the whole tree. Overall, this analysis allowed us to estimate the age composition of the



NSC reserves being used at any point of the source limitation event and the time that each tree would take to exhaust those reserves.

### ***Sensitivity of NSC mean age and mean transit time to changes in carbon allocation***

Along with carbon source variability, sink strength also plays a fundamental role in NSC dynamics of mature trees. This is reflected in the NSC mean age and mean transit time if the assimilation of carbon is kept constant and numerical changes are induced in the cycling rates between carbon pools. The sensitivity analysis estimated that the efflux rate of carbon from the storage in the stem and the cycling rates of roots have a large influence on the NSC mean age and mean transit time, playing an important role in NSC dynamics (Fig. S2). But, none of the carbon fluxes related to the foliage compartments had an important impact in the mean ages and transit time of the trees' NSC (Fig. S2). Previous studies have shown that stored NSC in the stem and roots contributes to the respired CO<sub>2</sub> of trees under stress (Carbone *et al.*, 2006; Richardson *et al.*, 2012; Muhr *et al.*, 2013, 2018; Hartmann *et al.*, 2018), and that stored carbon belowground is vital to tree recovery after a disturbance (Schutz *et al.*, 2009; Hagedorn *et al.*, 2016; McDowell *et al.*, 2018). These allocation rates usually change when trees experience limiting conditions (Nogués *et al.*, 2006; Wiley *et al.*, 2013, 2019; Hagedorn *et al.*, 2016), but the mechanism behind these changes remains uncertain (Chesney & Vasquez, 2007; Gaudinski *et al.*, 2009; Hartmann *et al.*, 2013; Mei *et al.*, 2015). When modeling carbon allocation as compartmental systems, we should be aware that changes in the fluxes between compartments can be due to changes in the compartment mass (mass conservation principle) or changes in the cycling rates (transfer coefficients of the matrix B) of the trees. In our simulations, the transfer coefficients remained constant, so changes

in the fluxes after the carbon limitation only reflected changes in the mass of the compartments. However, a change in NSC dynamics happens when the cycling rates change independently of the system carbon mass, which would change the carbon transfer coefficients between pools, as done in our sensitivity analysis. For instance, increasing the allocation rates from the storage in the wood to growth or respiration ( $C_s$ ) would make the trees to cycle carbon faster, build younger reserves during their productive and healthy conditions, and increase the tree's vulnerability to starvation; while increasing the allocation of carbon to storage in the roots ( $S_r$ ) would make them slower cyclers, build older reserves and be more resilient to low productivity periods (Fig. S3). Based on our models, we have estimated how cycling rates drive the NSC age and transit time distributions of mature trees.

## Limitations and conclusions

Comparisons between the estimated NSC mean age and mean transit time with empirical measurements can serve as important diagnostics for model evaluation (Ceballos-Núñez *et al.*, 2018). However, the models used here are not easy to parameterize and require a large number of observations. Our model parameters are rough estimates of the fluxes for an average healthy mature tree of each species (ACGCA model) or population of trees (*P. halepensis* case), and their structure may misrepresent other mechanisms. They are also constrained by the assumptions made when the parameters were estimated, e.g., the NSC allocation to storage happens passively when carbon supply exceeds demand. These parameter estimates can be improved with empirical research, theoretical studies, and statistical approaches that consider variability within and among trees as well as

alternative assumptions regarding NSC allocation. Furthermore, our representations are very simple and do not consider nonlinear interactions and other important fluxes, such as the exchange of carbon with the rhizosphere (Epron *et al.*, 2011), allocation of carbon to reproduction (Hacket-Pain *et al.*, 2018), emissions of biogenic volatile organic compounds (BVOC) (Epron *et al.*, 2012), and allocation to defense compounds (Huang *et al.*, 2019a), which also play an important role for determining NSC dynamics. However, information about these fluxes is still scarce and uncertain. Nevertheless, our results open the possibility to better understand NSC dynamics in mature trees based on estimated NSC ages and transit times in different tree organs of species with contrasting life strategies and growth environments. Our estimates are relevant for characterizing general differences in the NSC dynamics in contrasting tree species, identifying different storage traits based on plant type and growth environment; predicting how trees use their reserves under stress, e.g., the exponential-linear increase of the NSC transit time as trees exhaust their reserves; providing a plausible probabilistic interpretation about why trees consume primarily young carbon during healthy stages and why this shifts after a prolonged carbon limitation; and identifying the determinant sink fluxes in NSC dynamics for mature trees.

## Acknowledgements

We want to thank Markus Müller for important support given in writing the code for running the models and simulations. This work was supported by the GIF (German Israeli Fund) funding Grant number I-1334-307.8, the German Research Foundation through its Emmy Noether Program (SI 1953/2–1), and the German Centre for Integrative Biodiversity Research (iDiv) Halle-Jena-Leipzig, D- 04103 Leipzig.

## Author Contribution

CS and DH conceived the idea. All authors contributed with the design of the work. DH performed the computations and wrote the manuscript. All authors revised the manuscript and gave important and critical input.

## References

- Anderegg WRL, Anderegg LDL. 2013.** Hydraulic and carbohydrate changes in experimental drought-induced mortality of saplings in two conifer species. *Tree Physiology* **33**: 252–260.
- von Arx G, Arzac A, Fonti P, Frank D, Zweifel R, Rigling A, Galiano L, Gessler A, Olano JM. 2017.** Responses of sapwood ray parenchyma and non-structural carbohydrates of *Pinus sylvestris* to drought and long-term irrigation. *Functional Ecology* **31**: 1371–1382.
- Bolin B, Rodhe H. 1973.** A note on the concepts of age distribution and transit time in natural reservoirs. *Tellus* **25**: 58–62.
- Bréda N, Huc R, Granier A, Dreyer E. 2006.** Temperate forest trees and stands under severe drought: a review of ecophysiological responses, adaptation processes and long-term consequences. *Annals of Forest Science* **63**: 625–644.
- Campolongo F, Cariboni J, Saltelli A. 2007.** An effective screening design for sensitivity analysis of large models. *Environmental Modelling & Software* **22**: 1509–1518.
- Carbone MS, Czimczik CI, Keenan TF, Murakami PF, Pederson N, Schaberg PG,**

597 **Xu X, Richardson AD. 2013.** Age, allocation and availability of nonstructural carbon in  
 598 mature red maple trees. *New Phytologist* **200**: 1145–1155.

599 **Carbone MS, Czimczik CI, McDuffee KE, Trumbore SE. 2006.** Allocation and  
 600 residence time of photosynthetic products in a boreal forest using a low-level  $^{14}\text{C}$  pulse-  
 601 chase labeling technique. *Global Change Biology* **13**: 466–477.

602 **Carnicer J, Coll M, Ninyerola M, Pons X, Sanchez G, Penuelas J. 2011.** Widespread  
 603 crown condition decline, food web disruption, and amplified tree mortality with increased  
 604 climate change-type drought. *Proceedings of the National Academy of Sciences* **108**:  
 605 1474–1478.

606 **Ceballos-Núñez V, Richardson AD, Sierra CA. 2018.** Ages and transit times as  
 607 important diagnostics of model performance for predicting carbon dynamics in terrestrial  
 608 vegetation models. *Biogeosciences* **15**: 1607–1625.

609 **Chesney P, Vasquez N. 2007.** Dynamics of non-structural carbohydrate reserves in  
 610 pruned *Erythrina poeppigiana* and *Gliricidia sepium* trees. *Agroforestry Systems* **69**: 89–  
 611 105.

612 **Cuntz M, Mai J, Zink M, Thober S, Kumar R, Schäfer D, Schrön M, Craven J,**  
 613 **Rakovec O, Spieler D, et al. 2015.** Computationally inexpensive identification of  
 614 noninformative model parameters by sequential screening. *Water Resources Research* **51**:  
 615 6417–6441.

616 **D’Andrea E, Rezaie N, Battistelli A, Gavrichkova O, Kuhlmann I, Matteucci G,**  
 617 **Moscatello S, Proietti S, Scartazza A, Trumbore S, et al. 2019.** Winter’s bite: beech  
 618 trees survive complete defoliation due to spring late-frost damage by mobilizing old C  
 619 reserves. *New Phytologist* **224**: 625–631.

620 **Dietze MC, Sala A, Carbone MS, Czimczik CI, Mantooth JA, Richardson AD,**  
621 **Vargas R. 2014.** Nonstructural Carbon in Woody Plants. *Annual Review of Plant Biology*  
622 **65:** 667–687.

623 **Epron D, Bahn M, Derrien D, Lattanzi FA, Pumpanen J, Gessler A, Högberg P,**  
624 **Maillard P, Dannoura M, Gérant D, et al. 2012.** Pulse-labelling trees to study carbon  
625 allocation dynamics: a review of methods, current knowledge and future prospects. *Tree*  
626 *Physiology* **32:** 776–798.

627 **Epron D, Ngao J, Dannoura M, Bakker MR, Zeller B, Bazot S, Bosc A, Plain C,**  
628 **Lata JC, Priault P, et al. 2011.** Seasonal variations of belowground carbon transfer  
629 assessed by in situ  $^{13}\text{CO}_2$  pulse labelling of trees. *Biogeosciences* **8:** 1153–1168.

630 **Gaudinski JB, Torn MS, Riley WJ, Swanston C, Trumbore SE, Joslin JD, Majdi H,**  
631 **Dawson TE, Hanson PJ. 2009.** Use of stored carbon reserves in growth of temperate  
632 tree roots and leaf buds: analyses using radiocarbon measurements and modeling. *Global*  
633 *Change Biology* **15:** 992–1014.

634 **Hacket-Pain AJ, Ascoli D, Vacchiano G, Biondi F, Cavin L, Conedera M,**  
635 **Drobyshev I, Liñán ID, Friend AD, Grabner M, et al. 2018.** Climatically controlled  
636 reproduction drives interannual growth variability in a temperate tree species. *Ecology*  
637 *Letters* **21:** 1833–1844.

638 **Hagedorn F, Joseph J, Peter M, Luster J, Pritsch K, Geppert U, Kerner R, Molinier**  
639 **V, Egli S, Schaub M, et al. 2016.** Recovery of trees from drought depends on  
640 belowground sink control. *Nature Plants* **2:** 16111.

641 **Hartmann H, Adams HD, Hammond WM, Hoch G, Landhäusser SM, Wiley E,**  
642 **Zaehle S. 2018.** Identifying differences in carbohydrate dynamics of seedlings and

643 mature trees to improve carbon allocation in models for trees and forests. *Environmental*  
 644 *and Experimental Botany* **152**: 7–18.

645 **Hartmann H, Trumbore S. 2016.** Understanding the roles of nonstructural  
 646 carbohydrates in forest trees – from what we can measure to what we want to know. *New*  
 647 *Phytologist* **211**: 386–403.

648 **Hartmann H, Ziegler W, Trumbore S. 2013.** Lethal drought leads to reduction in  
 649 nonstructural carbohydrates in Norway spruce tree roots but not in the canopy.  
 650 *Functional Ecology* **27**: 413–427.

651 **Huang J, Forkelová L, Unsicker SB, Forkel M, Griffith DWT, Trumbore S,**  
 652 **Hartmann H. 2019a.** Isotope labeling reveals contribution of newly fixed carbon to  
 653 carbon storage and monoterpenes production under water deficit and carbon limitation.  
 654 *Environmental and Experimental Botany* **162**: 333–344.

655 **Huang J, Hammerbacher A, Weinhold A, Reichelt M, Gleixner G, Behrendt T, Dam**  
 656 **NM, Sala A, Gershenson J, Trumbore S, et al. 2019b.** Eyes on the future – evidence for  
 657 trade-offs between growth, storage and defense in Norway spruce. *New Phytologist* **222**:  
 658 144–158.

659 **IPCC. 2018.** *Summary for Policymakers. In: Global warming of 1.5°C. An IPCC*  
 660 *Special Report on the impacts of global warming of 1.5°C above pre-industrial levels and*  
 661 *related global greenhouse gas emission pathways, in the context of strengthening the*  
 662 *global response to the threat of climate change, sustainable development, and efforts to*  
 663 *eradicate poverty* (T Waterfield V, Masson-Delmotte P, Zhai, H O Pörtner, D Roberts, J  
 664 Skea, P R Shukla, A Pirani, W Moufouma-Okia, C Péan, R Pidcock, S Connors, J B R  
 665 Matthews, Y Chen, X Zhou, M I Gomis, E Lonnoy, T Maycock, M Tignor, Ed.). World

- 666 Meteorological Organization, Geneva.
- 667 **Jacquez JA, Simon CP. 1993.** Qualitative Theory of Compartmental Systems. *SIAM*  
 668 *Review* **35**: 43–79.
- 669 **Keel SG, Siegwolf RTW, Jäggi M, Körner C. 2007.** Rapid mixing between old and  
 670 new C pools in the canopy of mature forest trees. *Plant, Cell & Environment* **30**: 963–  
 671 972.
- 672 **Klein T, Hartmann H. 2018.** Climate change drives tree mortality (J Sills, Ed.). *Science*  
 673 **362**: 758.
- 674 **Klein T, Hoch G. 2015.** Tree carbon allocation dynamics determined using a carbon  
 675 mass balance approach. *New Phytologist* **205**: 147–159.
- 676 **Lacointe A, Deleens E, Ameglio T, Saint-Joanis B, Lelarge C, Vandame M, Song**  
 677 **GC, Daudet FA. 2004.** Testing the branch autonomy theory: a  $^{13}\text{C}/^{14}\text{C}$  double-labelling  
 678 experiment on differentially shaded branches. *Plant, Cell & Environment* **27**: 1159–1168.
- 679 **Martínez-Vilalta J, Sala A, Asensio D, Galiano L, Hoch G, Palacio S, Piper FI,**  
 680 **Lloret F. 2016.** Dynamics of non-structural carbohydrates in terrestrial plants: a global  
 681 synthesis. *Ecological Monographs* **86**: 495–516.
- 682 **McDowell N, Allen CD, Anderson-Teixeira K, Brando P, Brien R, Chambers J,**  
 683 **Christoffersen B, Davies S, Doughty C, Duque A, et al. 2018.** Drivers and mechanisms  
 684 of tree mortality in moist tropical forests. *New Phytologist* **219**: 851–869.
- 685 **Mei L, Xiong Y, Gu J, Wang Z, Guo D. 2015.** Whole-tree dynamics of non-structural  
 686 carbohydrate and nitrogen pools across different seasons and in response to girdling in  
 687 two temperate trees. *Oecologia* **177**: 333–344.
- 688 **Metzler H, Müller M, Sierra CA. 2018.** Transit-time and age distributions for nonlinear



689 time-dependent compartmental systems. *Proceedings of the National Academy of*  
690 *Sciences*.

691 **Metzler H, Sierra CA. 2018.** Linear Autonomous Compartmental Models as  
692 Continuous-Time Markov Chains: Transit-Time and Age Distributions. *Mathematical*  
693 *Geosciences* **50**: 1–34.

694 **Morris MD. 1991.** Factorial sampling plans for preliminary computational experiments.  
695 *Technometrics* **33**: 161–174.

696 **Muhr J, Angert A, Negrón-Juárez RI, Muñoz WA, Kraemer G, Chambers JQ,**  
697 **Trumbore SE. 2013.** Carbon dioxide emitted from live stems of tropical trees is several  
698 years old. *Tree Physiology* **33**: 743–752.

699 **Muhr J, Messier C, Delagrangé S, Trumbore S, Xu X, Hartmann H. 2016.** How fresh  
700 is maple syrup? Sugar maple trees mobilize carbon stored several years previously during  
701 early springtime sap-ascent. *New Phytologist* **209**: 1410–1416.

702 **Muhr J, Trumbore S, Higuchi N, Kunert N. 2018.** Living on borrowed time –  
703 Amazonian trees use decade-old storage carbon to survive for months after complete  
704 stem girdling. *New Phytologist* **220**: 111–120.

705 **Nogués S, Damesin C, Tcherkez G, Maunoury F, Cornic G, Ghashghaie J. 2006.**  
706  $^{13}\text{C}/^{12}\text{C}$  isotope labelling to study leaf carbon respiration and allocation in twigs of field-  
707 grown beech trees. *Rapid Communications in Mass Spectrometry* **20**: 219–226.

708 **Nunez S, Arets E, Alkemade R, Verwer C, Leemans R. 2019.** Assessing the impacts of  
709 climate change on biodiversity: is below 2 °C enough? *Climatic Change* **154**: 351–365.

710 **Ogle K, Pacala SW. 2009.** A modeling framework for inferring tree growth and  
711 allocation from physiological, morphological and allometric traits. *Tree Physiology* **29**:

- 712 587–605.
- 713 **Oliveira AS, Rajão RG, Soares Filho BS, Oliveira U, Santos LRS, Assunção AC,**  
 714 **Hoff R, Rodrigues HO, Ribeiro SMC, Merry F, *et al.* 2019.** Economic losses to  
 715 sustainable timber production by fire in the Brazilian Amazon. *The Geographical Journal*  
 716 **185:** 55–67.
- 717 **Overdieck D. 2016.** Nonstructural and Structural Carbohydrates. In: CO<sub>2</sub>, Temperature,  
 718 and Trees: Experimental Approaches. Singapore: Springer Singapore, 65–79.
- 719 **Parkinson S, Young P. 1998.** Uncertainty and sensitivity in global carbon cycle  
 720 modelling. *Climate Research* **9:** 157–174.
- 721 **Pugh TAM, Lindeskog M, Smith B, Poulter B, Arneth A, Haverd V, Calle L. 2019.**  
 722 Role of forest regrowth in global carbon sink dynamics. *Proceedings of the National*  
 723 *Academy of Sciences* **116:** 4382.
- 724 **Pujol G, Iooss B, Boumhaout AJ with contributions from K, Veiga SD, Delage T,**  
 725 **Fruth J, Gilquin L, Guillaume J, Gratiot LL, Lemaitre P, *et al.* 2017.** *Sensitivity:*  
 726 *Global Sensitivity Analysis of Model Outputs.*
- 727 **Richardson AD, Carbone MS, Huggett BA, Furze ME, Czimczik CI, Walker JC, Xu**  
 728 **X, Schaberg PG, Murakami P. 2015.** Distribution and mixing of old and new  
 729 nonstructural carbon in two temperate trees. *New Phytologist* **206:** 590–597.
- 730 **Richardson AD, Carbone MS, Keenan TF, Czimczik CI, Hollinger DY, Murakami**  
 731 **P, Schaberg PG, Xu X. 2012.** Seasonal dynamics and age of stemwood nonstructural  
 732 carbohydrates in temperate forest trees. *New Phytologist* **197:** 850–861.
- 733 **Schutz AEN, Bond WJ, Cramer MD. 2009.** Juggling carbon: allocation patterns of a  
 734 dominant tree in a fire-prone savanna. *Oecologia* **160:** 235–246.

- Sierra CA, Müller M, Trumbore SE. 2014.** Modeling radiocarbon dynamics in soils: SoilR version 1.1. *Geosci. Model Dev.* **7**: 1919–1931.
- Strand J. 2017.** Modeling the marginal value of rainforest losses: A dynamic value function approach. *Ecological Economics* **131**: 322–329.
- Trugman AT, Detto M, Bartlett MK, Medvigy D, Anderegg WRL, Schwalm C, Schaffer B, Pacala SW. 2018.** Tree carbon allocation explains forest drought-kill and recovery patterns. *Ecology Letters* **21**: 1552–1560.
- Trumbore S, Czimczik CI, Sierra CA, Muhr J, Xu X. 2015.** Non-structural carbon dynamics and allocation relate to growth rate and leaf habit in California oaks. *Tree Physiology* **35**: 1206–1222.
- Vargas R, Trumbore SE, Allen MF. 2009.** Evidence of old carbon used to grow new fine roots in a tropical forest. *New Phytologist* **182**: 710–718.
- Wiley E, Huepenbecker S, Casper BB, Helliker BR. 2013.** The effects of defoliation on carbon allocation: can carbon limitation reduce growth in favour of storage? *Tree Physiology* **33**: 1216–1228.
- Wiley E, King CM, Landhäusser SM. 2019.** Identifying the relevant carbohydrate storage pools available for remobilization in aspen roots (D Tissue, Ed.). *Tree Physiology* **39**: 1109–1120.}

## Figures and tables

**Figure 1:** Compartmental representation for the carbon allocation model proposed for the evergreen Mediterranean *Pinus halepensis* by Klein and Hoch (2015). The square

compartments define the state variables, and the arrows define the fraction of carbon that is transferred between pools. The name and values of the fluxes and state variables are defined in the Tables 1 and 2. This model is described by the Equation 1.

**Figure 2:** Compartmental representation for carbon allocation proposed for the temperate deciduous *Acer rubrum* and evergreen *Pinus taeda* species based on a theoretical interpretation of the "ACGCA" developed by Ogle and Pacala (2009). The square compartments define the state variables, and the arrows define the fraction of carbon that is transferred between pools. The name of the fluxes and state variables are defined in the Tables 1 and 2. This model is described by the Equation 1

**Figure 3:** Age distribution of the non-structural carbon in the whole tree and the tree pools for each species *Pinus halepensis*, *Acer rubrum* and *Pinus taeda*. The frequencies are given in grams of carbon and the sum of all the frequencies of all the compartments is equal to the total mass of carbon of the system.

**Figure 4:** Age distribution of the non-structural carbon in the whole tree for years subsequent to the start of the carbon limitation simulation (years after disturbance) for each of the species *Pinus halepensis*, *Acer rubrum* and *Pinus taeda*.

**Figure 5:** Backward transit time distribution of the non-structural carbon in the whole tree during healthy conditions (Year 0 after disturbance) and years subsequent to the start of the simulated carbon limitation for each of the species *Pinus halepensis*, *Acer rubrum* and *Pinus taeda*.

**Figure 6:** Non-structural carbon mean backward transit time and the percentage of NSC

consumption during 50 years of the simulation for each species *Pinus halepensis*, *Acer rubrum* and *Pinus taeda*. The first 10 years of the simulation represent the steady state, with trees growing under healthy conditions. After this, assimilation was set to zero to simulate carbon limitation for the subsequent 40 years. For a given time step of the simulation there is a level of consumption given by the green line and specified in the right axis, and there is a backward transit time given by the blue line and noted in the left axis. This means backward transit time reflects the mean age of the carbohydrates being used in metabolism and growth in each time step of the simulations.

**Table 1:** Compartments names of the models described in Figs 1 and 2.

| Abbreviation | Name   |
|--------------|--|
| E            | Transient Carbon Pool                                  |
| FANSC        | Foliage Active Non Structural Carbon                   |
| FSNSC        | Foliage Stored Non Structural Carbon                   |
| FB           | Foliage Biomass  |
| BRANSC       | Branches and Coarse Roots Active Non Structural Carbon |
| BRB          | Branches and Coarse Roots Biomass                      |
| SANSC        | Stem Active Non Structural Carbon                      |
| SB           | Stem Biomass   |

|       |   |
|-------|---|
| SSNSC | Stem stored Non Structural carbon       |
| RANSC | Fine Roots Active Non Structural Carbon |
| RSNSC | Fine Roots Stored Non Structural Carbon |
| RB    | Fine Root Biomass                       |

793

794 **Table 2:** Annual mean and standard deviation (sd) of the carbon transfer coefficients  
795 (year<sup>-1</sup>) for the models in Figs. 1 and 2 for the species *Pinus halepensis* (model from  
796 Klein and Hoch 2015), *Acer rubrum* and *Pinus taeda* (ACGCA model from Ogle and  
797 Pacala 2009). Pool name abbreviations are defined in Table 1

| Abbreviation | Parameter Name                   | <i>P. halepensis</i> |       | <i>A. rubrum</i> |          | <i>P. taeda</i> |       |
|--------------|----------------------------------|----------------------|-------|------------------|----------|-----------------|-------|
|              |                                  | mean                 | sd    | mean             | sd       | mean            | sd    |
| A            | Assimilation at steady state     | 23520                |       | 211770           |          | 200090          |       |
| Rm           | Maintenance respiration          |                      |       | 0.25             | 0.053    | 0.167           | 0.033 |
| Fl           | Allocation to FANSC              |                      |       | 0.05             | 0.004    | 0.042           | 0.011 |
| BRl          | Allocation to BRANSC             |                      |       | 0.669            | 0.054    | 0.757           | 0.044 |
| Sl           | Allocation to SANSC              |                      |       | 1.00E-04         | 3.00E-03 | 6.24E-06        | 0.004 |
| Rl           | Allocation to RANSC              |                      |       | 0.031            | 0.006    | 0.035           | 0.016 |
| Rf           | Respiration foliage              | 9.56                 | 0.72  |                  |          |                 |       |
| Rbr          | Respiration branches and roots   |                      |       |                  |          |                 |       |
| Rs           | Respiration stem                 | 0.59                 | 0.026 |                  |          |                 |       |
| Rr           | Respiration roots                | 16.84                | 0.23  |                  |          |                 |       |
| Gf           | Growth foliage                   | 2.94                 | 0.05  | 0.939            | 0.003    | 0.932           | 0.015 |
| Gbr          | Growth branches and coarse roots |                      |       | 0.912            | 0.001    | 0.943           | 0.007 |
| Gs           | Growth stem                      | 0.3                  | 0.02  | 0.912            | 0.001    | 0.943           | 0.007 |
| Gr           | Growth roots                     | 1.28                 | 0.21  | 0.893            | 0.026    | 0.942           | 0.019 |
| Lf           | Litterfall foliage               | 0.34                 | 0.07  | 1                | 0        | 0.333           | 0.089 |
| Lbr          | Litterfall branches and roots    |                      |       | 0.047            | 0.021    | 0.047           | 0.018 |

|      |  |       |        |       |       |       |       |
|------|--|-------|--------|-------|-------|-------|-------|
| Lr   | Literfall fine roots   | 0.07  | 0.01   | 1     | 0.055 | 0.5   | 0.21  |
| LSs  | Stored NSC lost in wood conversion to heartwood and litter fall      | 0.003 | 0.0005 | 0.031 | 0.007 | 0.06  | 0.006 |
| Sf   | Allocation to storage in foliage (FSNSC)                             | 0.44  | 0.4    | 0.061 | 0.003 | 0.068 | 0.015 |
| Sbr  | Allocation to storage in stem from branches and coarse roots (SSNSC) |       |        | 0.088 | 0.001 | 0.057 | 0.007 |
| Ss   | Allocation to storage in stem (SSNSC)                                | 0.8   | 0.05   | 0.088 | 0.001 | 0.057 | 0.007 |
| Sr   | Allocation to storage in roots (RSNSC)                               | 4.98  | 2.64   | 0.107 | 0.026 | 0.058 | 0.019 |
| Cf   | Allocation from storage in foliage (FSNSC) to E                      | 2.02  | 0.68   | 1     | 0     | 0.333 | 0.089 |
| Cs   | Allocation from storage in stem (SSNSC) to E                         | 1.09  | 0.7    | 0.023 | 0.01  | 0.023 | 0.009 |
| Cr   | Allocation from storage in roots (RSNSC) to E                        | 1.22  | 0.58   | 1     | 0.055 | 0.5   | 0.21  |
| FtoS | Allocation from foliage to stem                                      | 33.7  | 3.2    |       |       |       |       |
| StoF | Allocation from stem to foliage                                      | 0.04  | 0.043  |       |       |       |       |
| Stor | Allocation from stem to roots  | 3.15  | 0.86   |       |       |       |       |
| rtoS | Allocation from roots to stem  | 0.11  | 0.11   |       |       |       |       |

**Table 3:** Mean ages for the different carbon pools in *Pinus halepensis*, *Acer rubrum* and *Pinus taeda* in units of years.

| Pool name | <i>P. halepensis</i> | <i>A. rubrum</i> | <i>P. taeda</i> |
|-----------|----------------------|------------------|-----------------|
| NSC tree  | 0.98 ± 0.38          | 9.45 ± 3.7       | 4.4 ± 0.72      |
| Ev        |                      | 1.55 ± 0.20      | 1.19 ± 0.06     |
| FANSC     | 0.03 ± 0.001         | 2.55 ± 0.20      | 2.19 ± 0.06     |
| FSNSC     | 0.52 ± 0.001         | 3.56 ± 0.20      | 5.22 ± 0.06     |
| SANSC     | 0.045 ± 0.10         | 2.55 ± 0.20      | 2.19 ± 0.06     |

|       |                  |                 |                  |
|-------|------------------|-----------------|------------------|
| SSNSC | $1.370 \pm 0.58$ | $21.3 \pm 5.38$ | $14.22 \pm 1.63$ |
| RANSC | $0.730 \pm 0.76$ | $2.55 \pm 0.20$ | $2.19 \pm 0.06$  |
| RSNSC | $1.550 \pm 0.12$ | $3.55 \pm 0.20$ | $4.19 \pm 0.06$  |

**Table 4:** Mean ages for the different organ specific pools in *Pinus halepensis*, *Acer rubrum* and *Pinus taeda* in units of years.

| Organ  | <i>P. halepensis</i> | <i>A. rubrum</i> | <i>P. taeda</i> |
|--------|----------------------|------------------|-----------------|
| Leaves | $0.07 \pm 0.001$     | $1.98 \pm 0.20$  | $1.91 \pm 0.06$ |
| Stem   | $0.73 \pm 0.580$     | $9.97 \pm 5.38$  | $4.58 \pm 1.63$ |
| Roots  | $1.33 \pm 0.760$     | $2.01 \pm 0.20$  | $2.36 \pm 0.06$ |

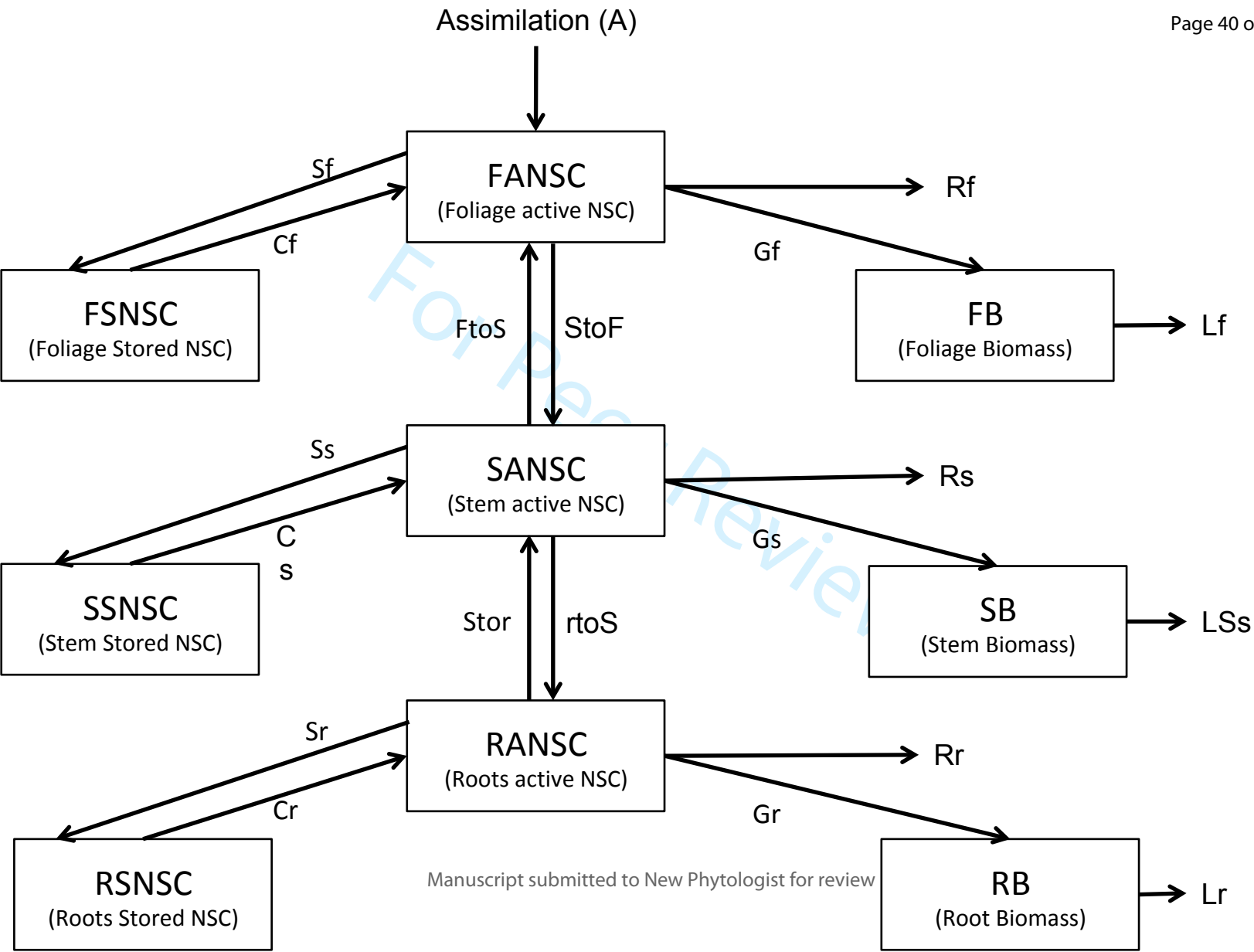
**Supporting information**

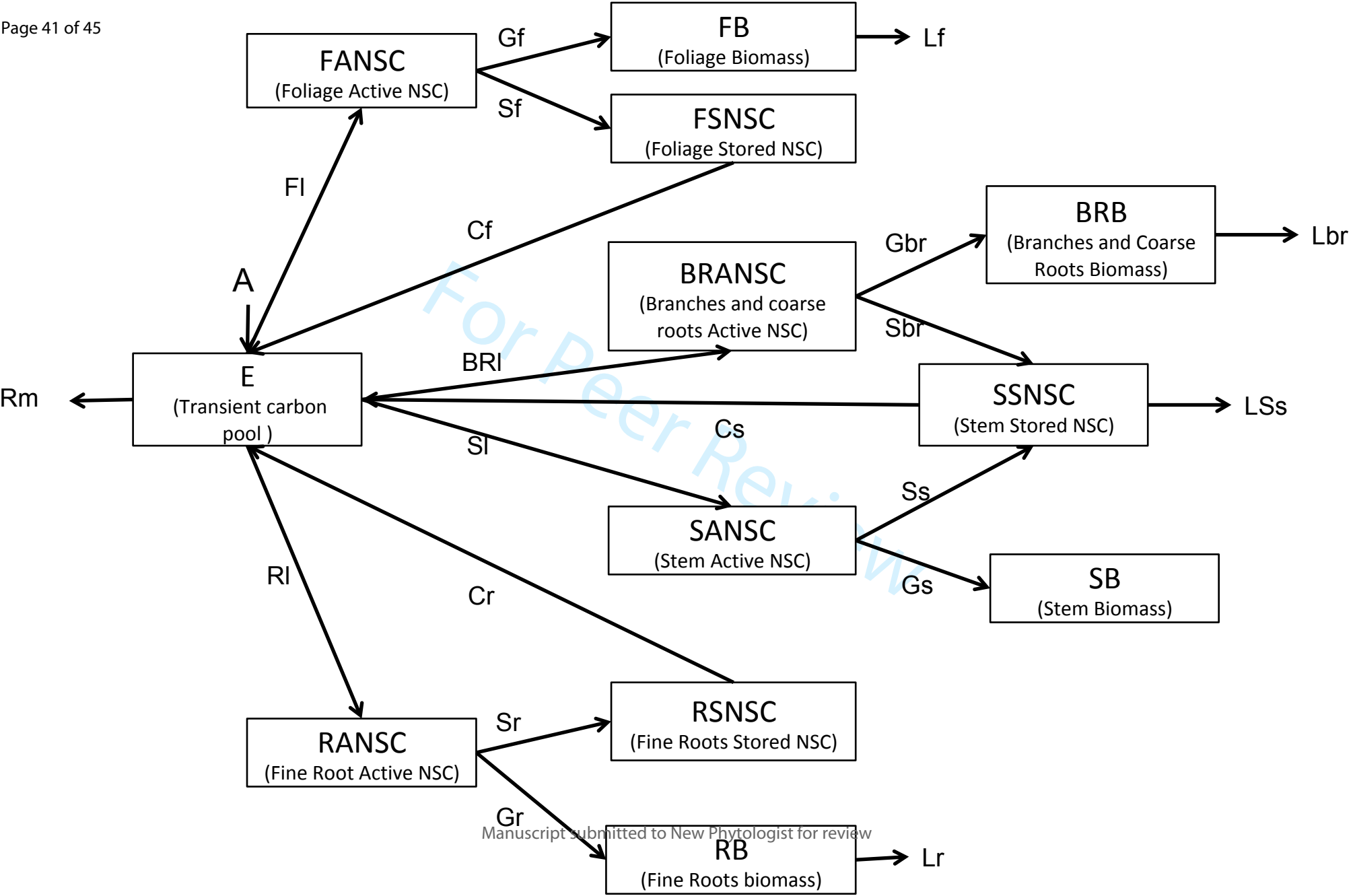
**Figure S1.** Uncertainties associated with the model parameters with the largest influence in the NSC mean age and mean transit time per species **a)** *Pinus halepensis*, **b)** *Acer rubrum*, and **c)** *Pinus taeda*.

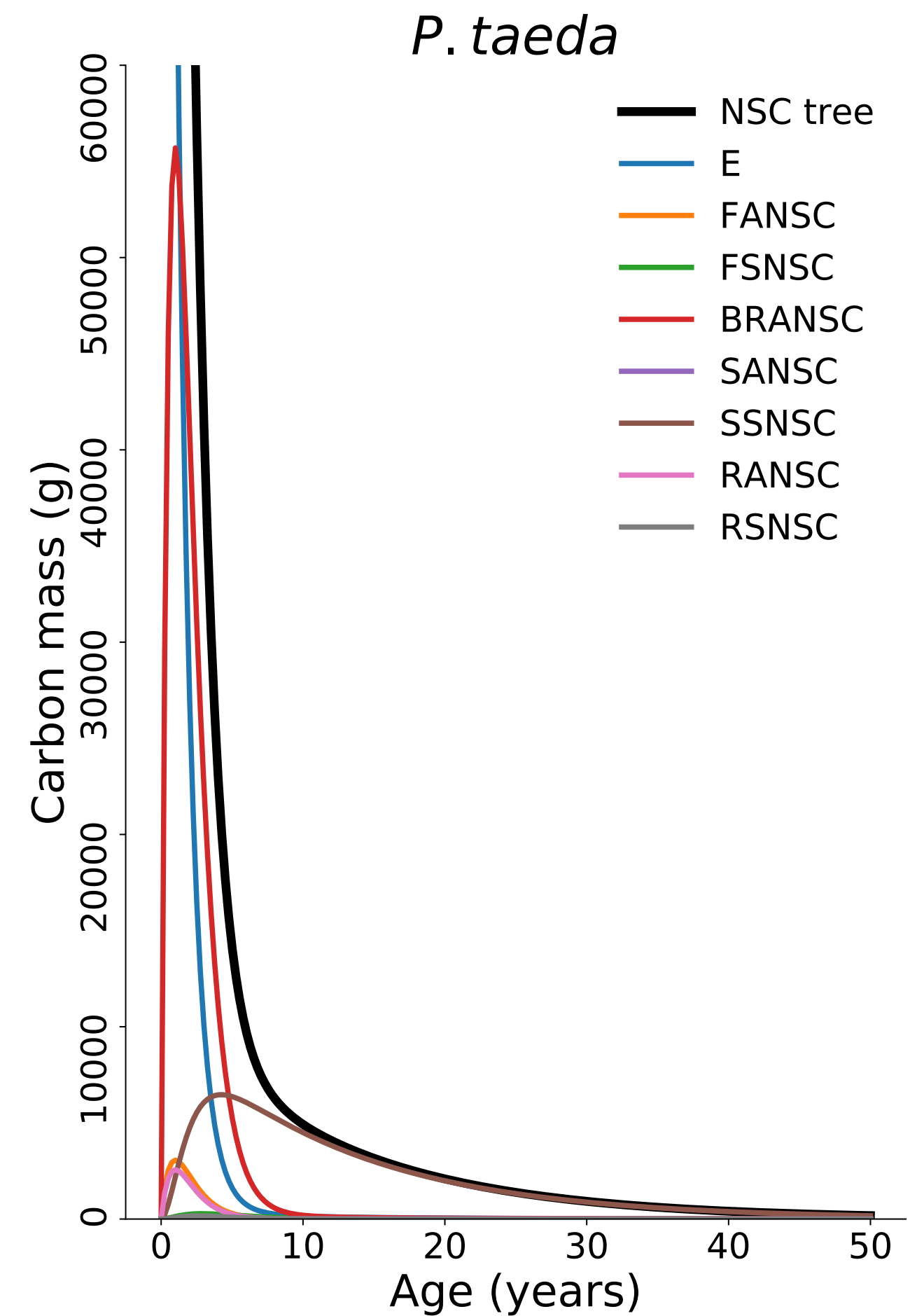
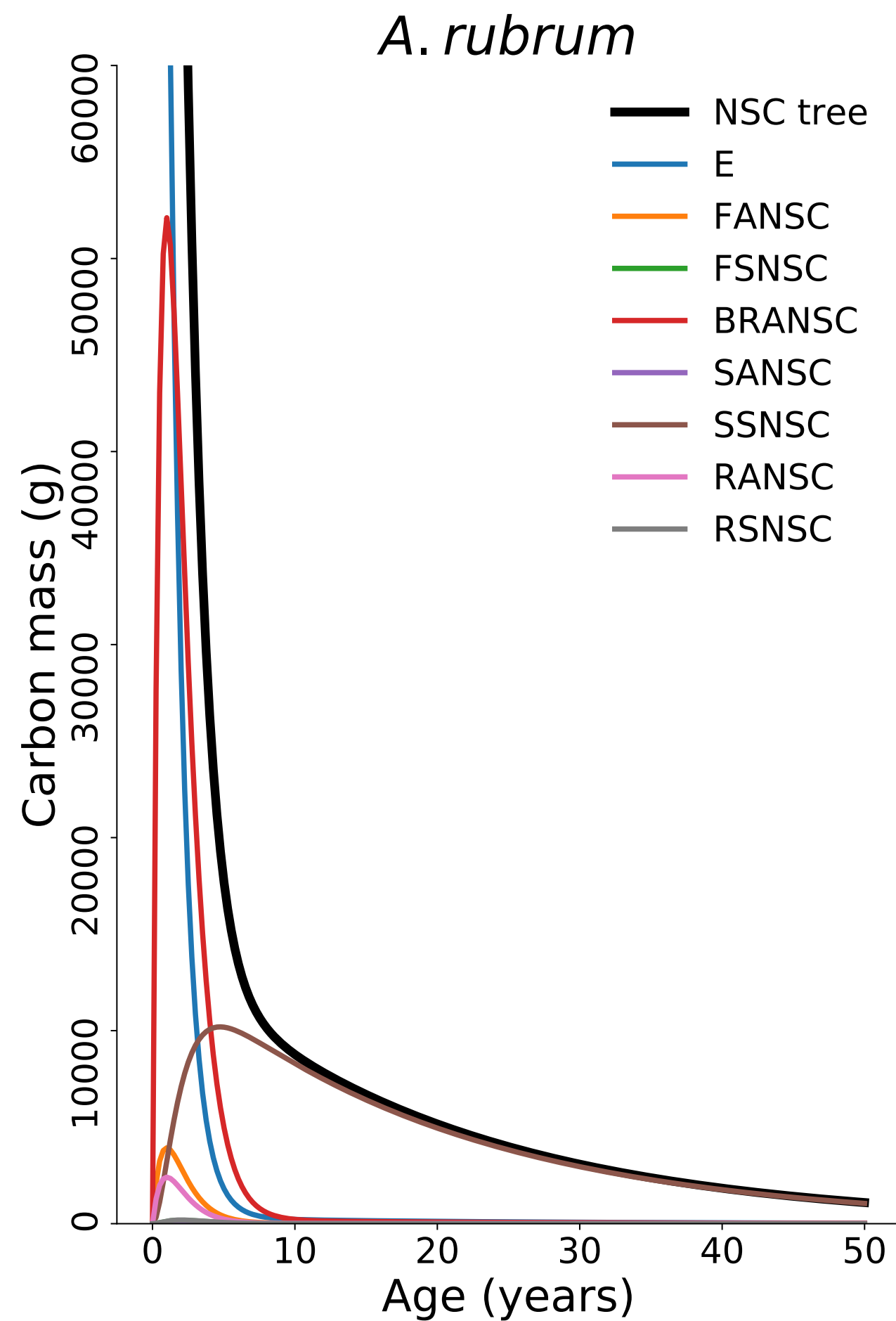
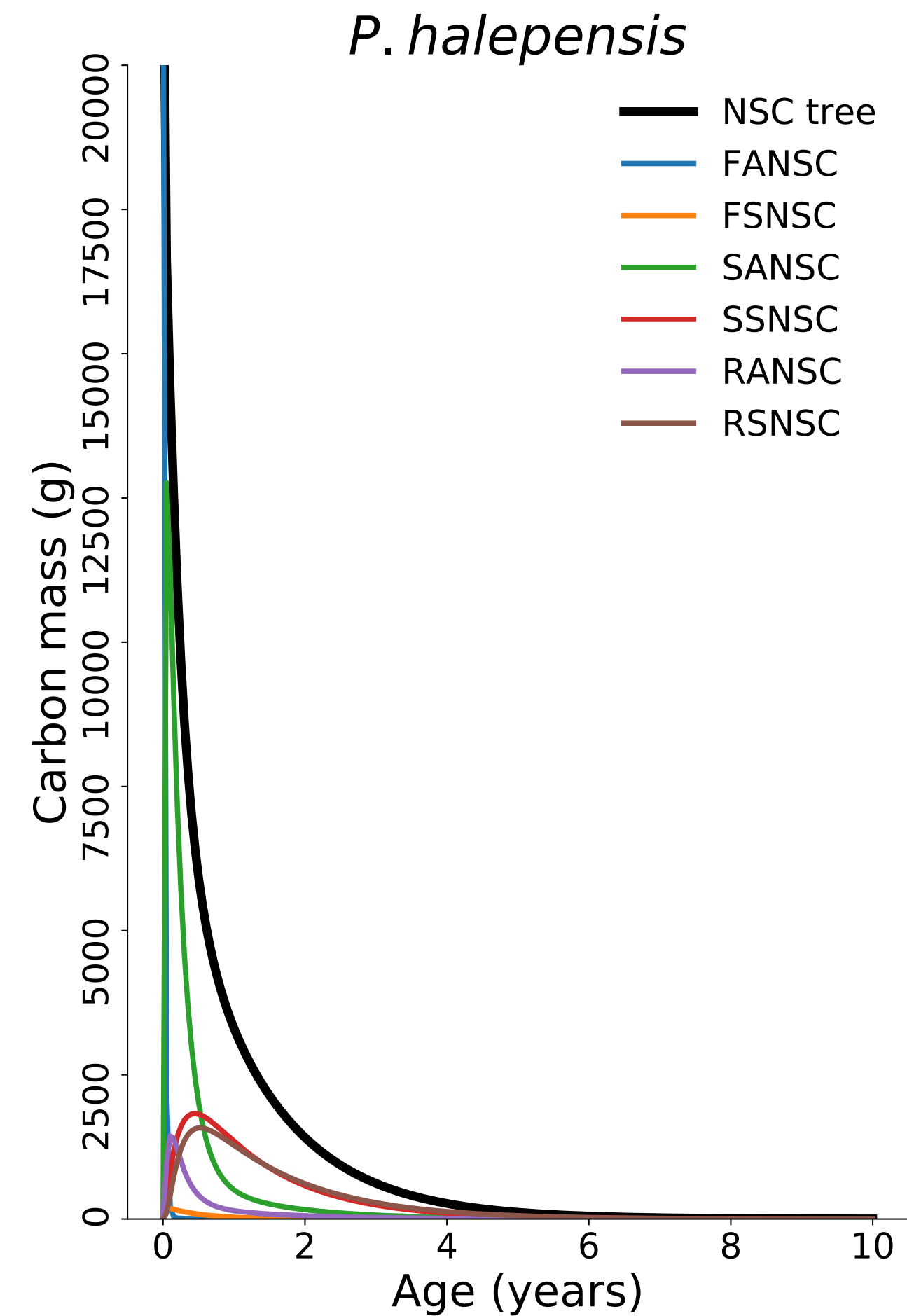
**Figure S2.** Mean sensitivity value  $\mu$  and its correspondent variance  $\sigma$  for each flux of each species (*Pinus halepensis*, *Acer rubrum* and *Pinus taeda*) calculated by the Elementary Effects method.

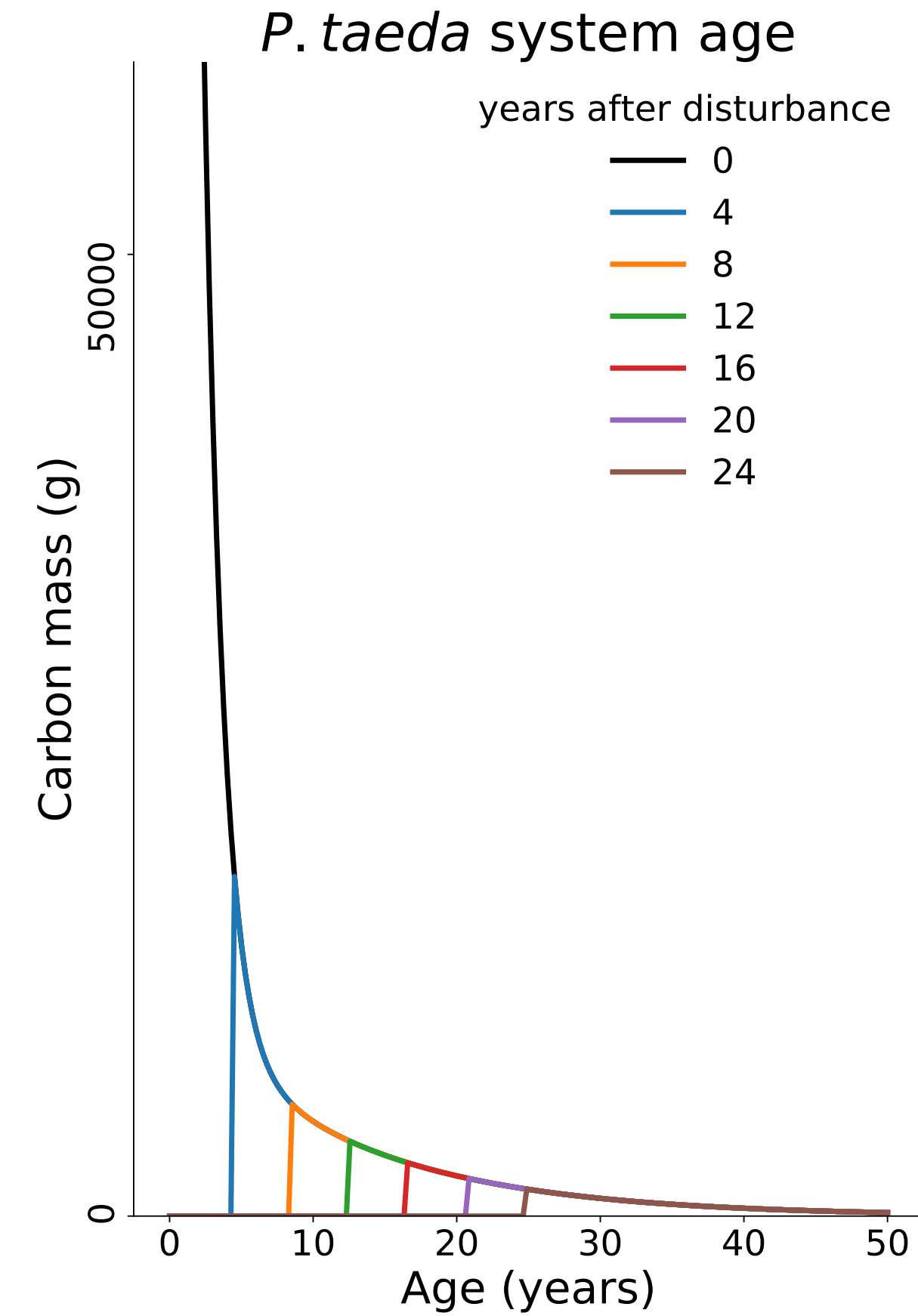
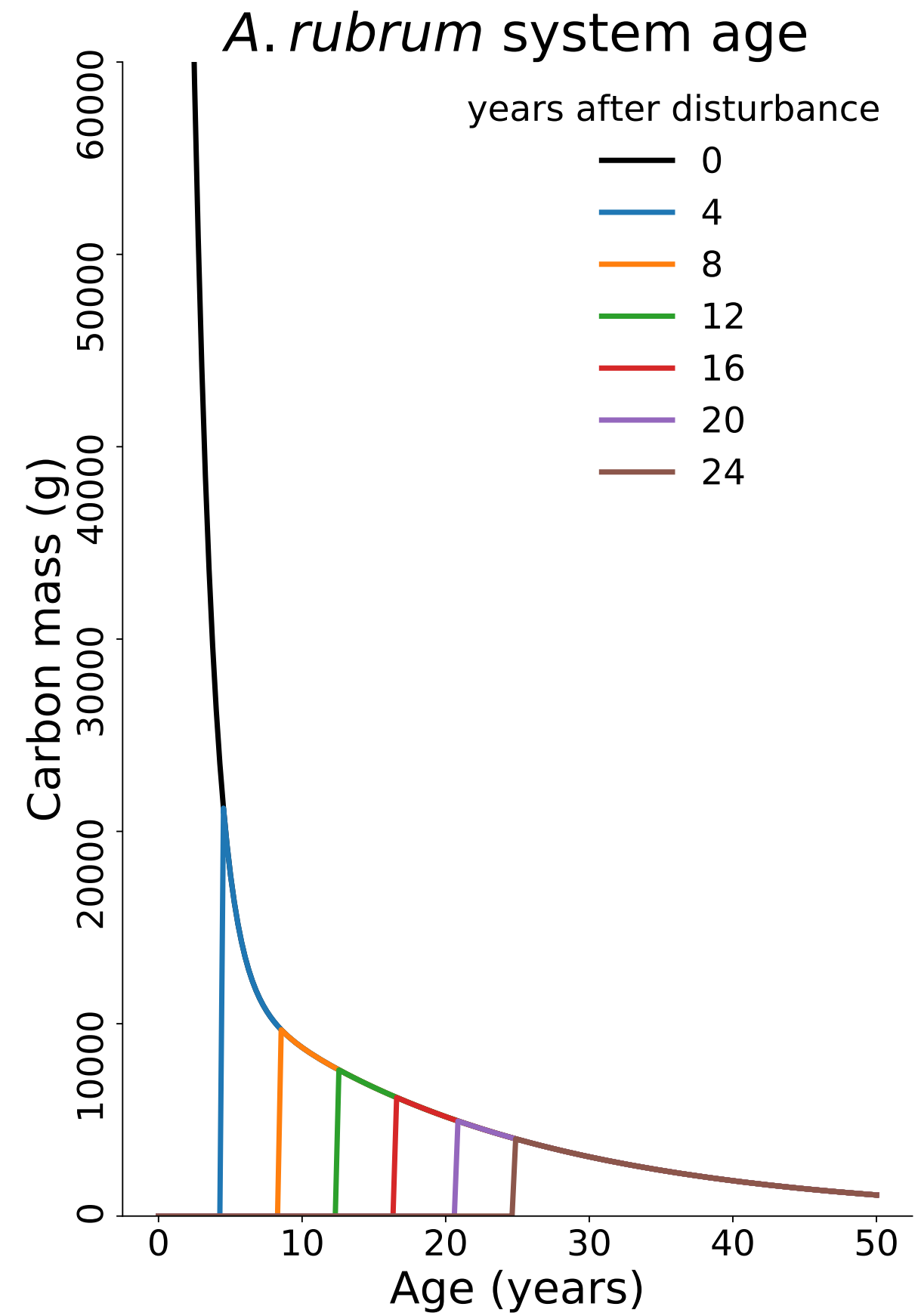
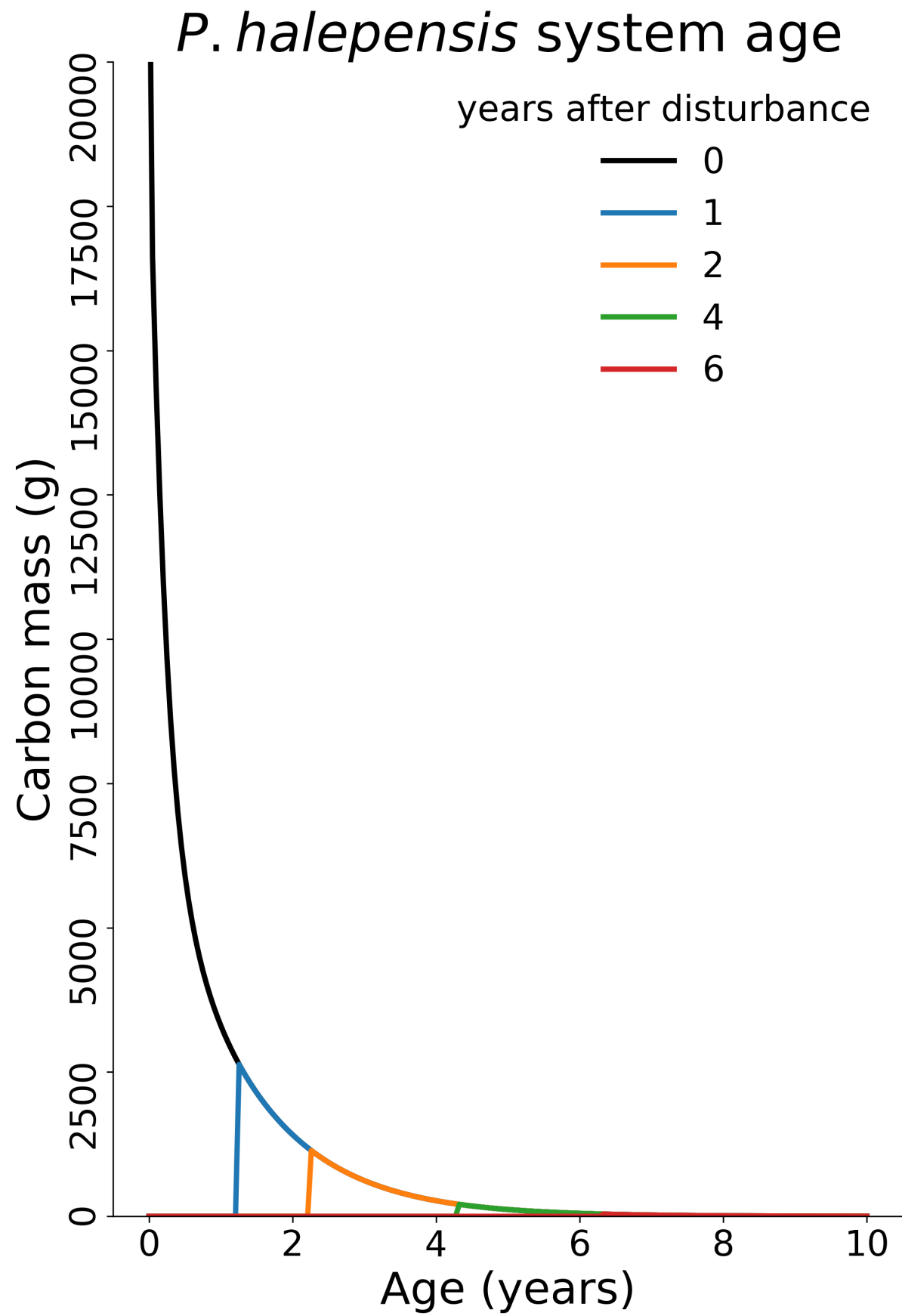
**Figure S3:** Association between the most sensitive NSC fluxes (Figure S2) and the mean age and mean transit time for each species: *Pinus halepensis*, *Acer rubrum* and *Pinus taeda*.

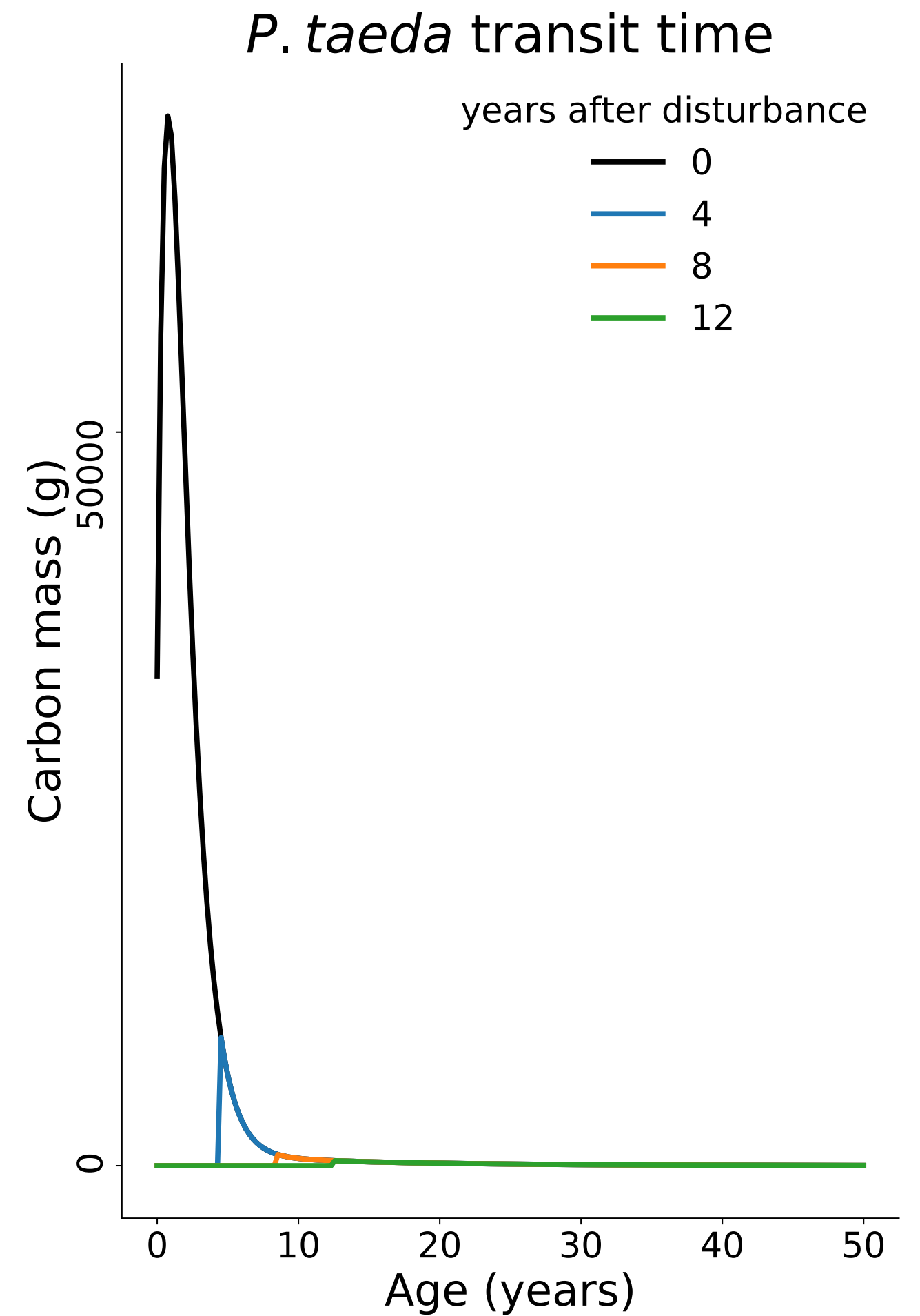
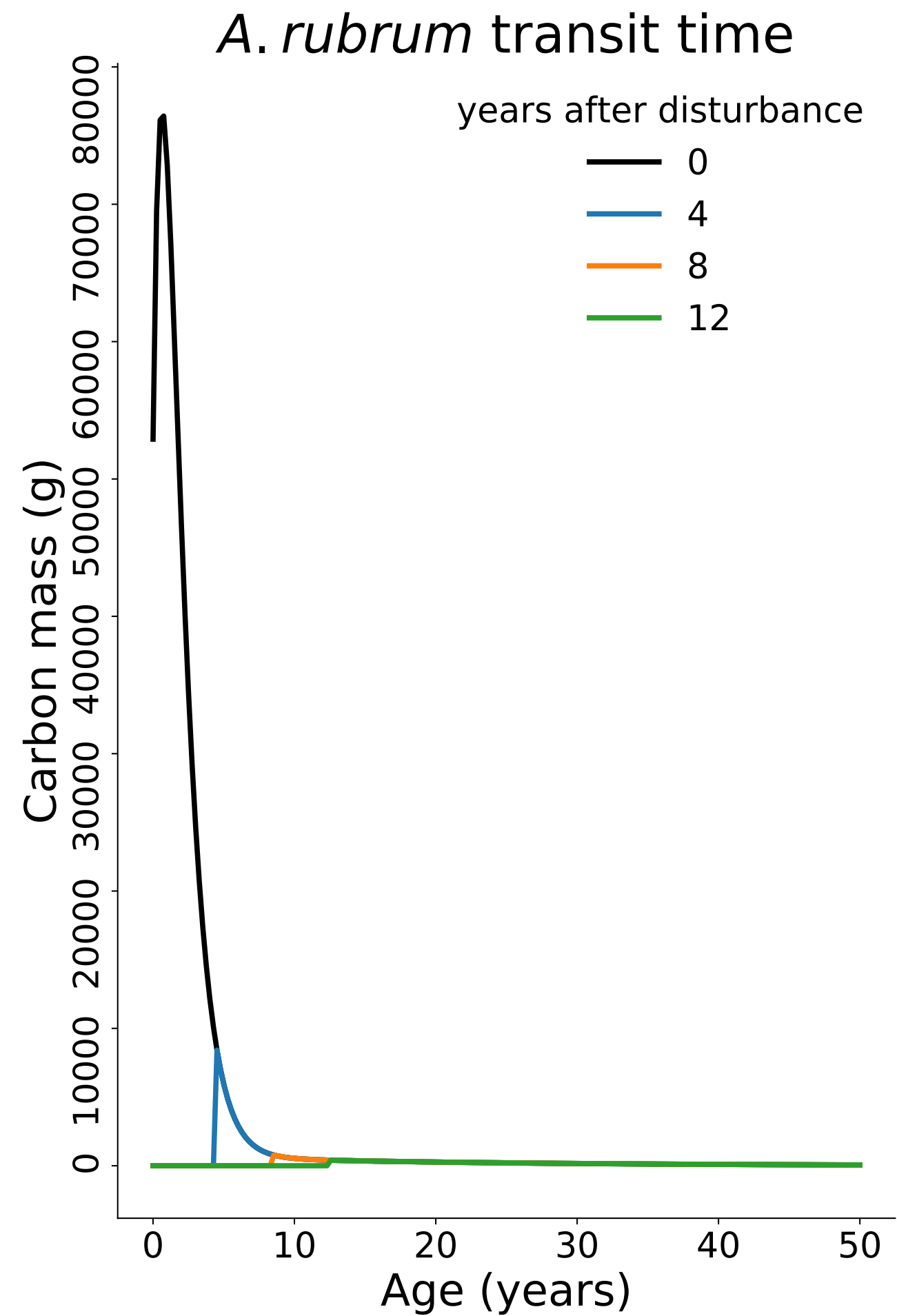
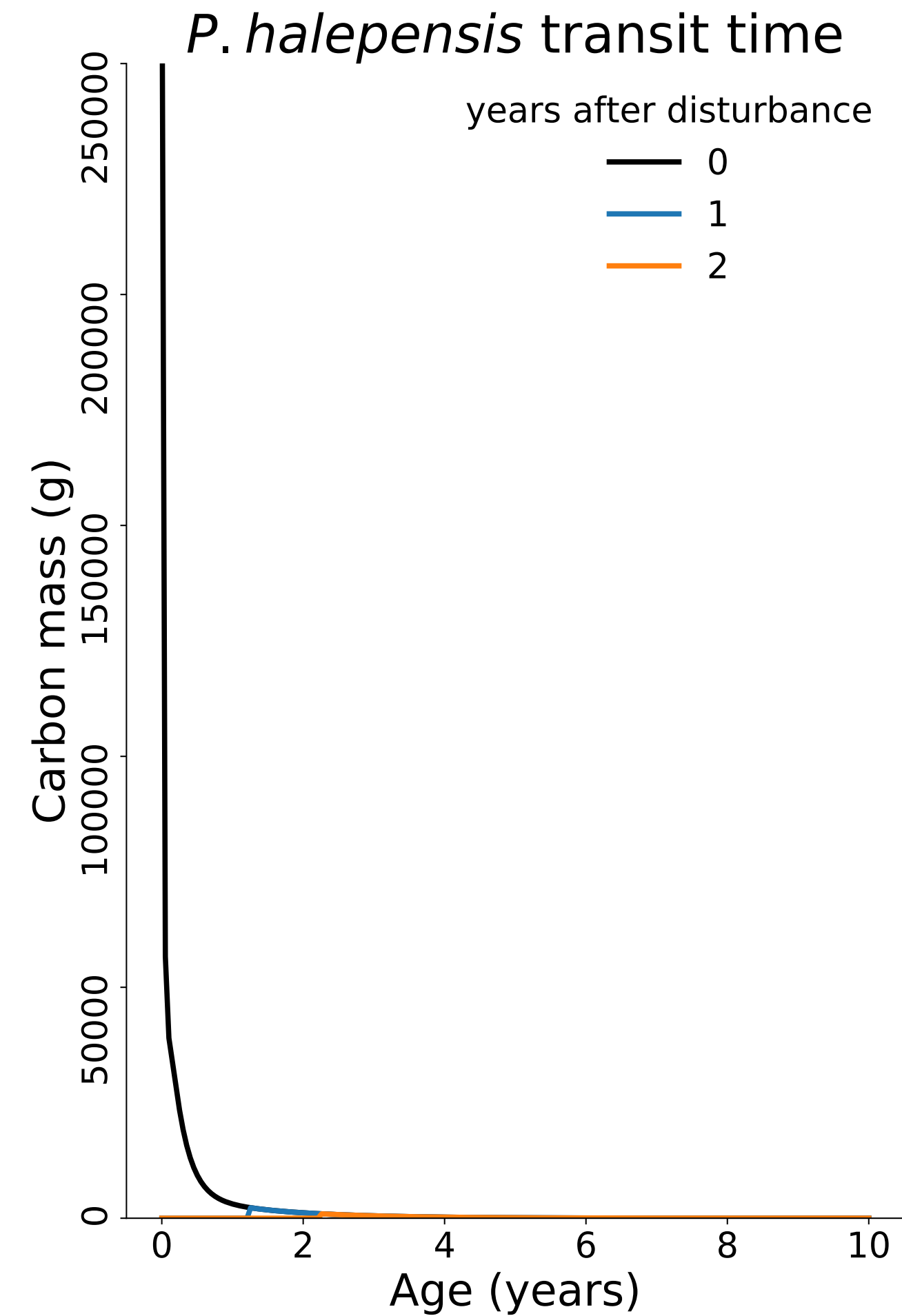












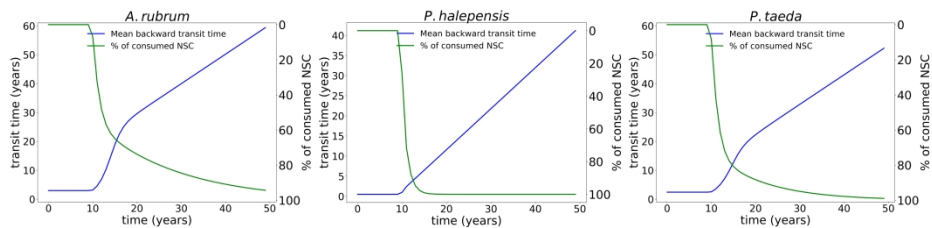


Figure 6: Non-structural carbon mean backward transit time and the percentage of NSC consumption during 50 years of the simulation for each species *Pinus halepensis*, *Acer rubrum* and *Pinus taeda*. The first 10 years of the simulation represent the steady state, with trees growing under healthy conditions. After this, assimilation was set to zero to simulate carbon limitation for the subsequent 40 years. For a given time step of the simulation there is a level of consumption given by the green line and specified in the right axis, and there is a backward transit time given by the blue line and noted in the left axis. This means backward transit time reflects the mean age of the carbohydrates being used in metabolism and growth in each time step of the simulations.

1707x616mm (72 x 72 DPI)